Interaction between repressor Opi1p and ER membrane protein Scs2p facilitates transit of phosphatidic acid from the ER to mitochondria and is essential for *INO1* gene expression in the presence of choline

Received for publication, August 2, 2017, and in revised form, September 8, 2017 Published, Papers in Press, September 18, 2017, DOI 10.1074/jbc.M117.809970

Maria L. Gaspar[1], **Yu-Fang Chang**[1,2], **Stephen A. Jesch, Manuel Aregullin, and Susan A. Henry**[3]

From the Department of Molecular Biology and Genetics, Cornell University, Ithaca, New York 14853

Edited by George M. Carman

In the yeast *Saccharomyces cerevisiae*, the Opi1p repressor controls the expression of *INO1* via the Opi1p/Ino2p–Ino4p regulatory circuit. Inositol depletion favors Opi1p interaction with both Scs2p and phosphatidic acid at the endoplasmic reticulum (ER) membrane. Inositol supplementation, however, favors the translocation of Opi1p from the ER into the nucleus, where it interacts with the Ino2p–Ino4p complex, attenuating transcription of *INO1*. A strain devoid of Scs2p (*scs2*Δ) and a mutant, *OPI1FFAT*, lacking the ability to interact with Scs2p were utilized to examine the specific role(s) of the Opi1p–Scs2p interaction in the regulation of *INO1* expression and overall lipid metabolism. Loss of the Opi1p–Scs2p interaction reduced *INO1* expression and conferred inositol auxotrophy. Moreover, inositol depletion in strains lacking this interaction resulted in Opi1p being localized to sites of lipid droplet formation, coincident with increased synthesis of triacylglycerol. Supplementation of choline to inositol-depleted growth medium led to decreased TAG synthesis in all three strains. However, in strains lacking the Opi1p–Scs2p interaction, Opi1p remained in the nucleus, preventing expression of *INO1*. These data support the conclusion that a specific pool of phosphatidic acid, associated with lipid droplet formation in the perinuclear ER, is responsible for the initial rapid exit of Opi1p from the nucleus to the ER and is required for *INO1* expression in the presence of choline. Moreover, the mitochondria-specific phospholipid, cardiolipin, was significantly reduced in both strains compromised for Opi1p–Scs2p interaction, indicating that this interaction is required for the transfer of phosphatidic acid from the ER to the mitochondria for cardiolipin synthesis.

Many genes encoding enzymes involved in glycerolipid biosynthesis (Fig. 1) in the yeast, *Saccharomyces cerevisiae*, contain the UAS_{INO} promoter element and are, thus, subject to coordinated transcriptional regulation in response to the availability of the phospholipid precursor, inositol, and, to a lesser degree, choline (1–5). UAS_{INO}-containing genes are repressed in yeast cells growing in the presence of exogenous inositol and, to a somewhat greater extent, when choline is also present in the medium (6–9). However, inositol and choline enter the pathway for phospholipid biosynthesis by entirely different pathways (Fig. 1) and impact regulation of lipid metabolism in distinctly different ways (2, 3, 6), a major topic addressed further in this paper. *INO1*, encoding *myo*-inositol-3-phosphate synthase (10), is the most highly regulated of the UAS_{INO}-containing genes (3–5, 8, 11), and its expression is essential for growth in the absence of exogenous inositol (12). The Ino2p–Ino4p activation complex binds to UAS_{INO} and is required for activation of *INO1* transcription in the absence of exogenous inositol (4, 13). Thus, *ino2*Δ and *ino4*Δ mutants are unable to activate *INO1* transcription and, consequently, exhibit stringent inositol auxotrophy (Ino^- phenotype), comparable with that of the *ino1*Δ mutant (Fig. 2) (3, 4, 14).

Regulated expression of *INO1* and other UAS_{INO}-containing genes, in response to inositol availability, is controlled by the cellular location of the Opi1p repressor (3, 4, 15). In wild-type cells growing in the absence of exogenous inositol, the Opi1p repressor is retained in the ER,[4] in part through its interaction with PA (15), precursor to PI and other phospholipids (Fig. 1). In the absence of exogenous inositol, yeast cells must rely on endogenous synthesis of inositol, catalyzed by inositol 3-phosphate synthase (Ino1p) (Fig. 1). Under these conditions, PI synthesis is reduced, leading to elevated PA levels and retention of Opi1p in the ER, thereby activating transcription of *INO1* and other UAS_{INO}-containing genes (3, 4, 11). However, when inositol is resupplied to inositol-depleted cultures, PI synthesis rapidly increases, PA levels decline, and Opi1p enters the nucleus (15). Once in the nucleus, Opi1p interacts with the transcriptional activation domain of the Ino2p activator, repressing expression of *INO1* (15) and other UAS_{INO}-containing genes (3–5, 11, 16).

This work was supported by National Institutes of Health Grant GM-19629 (to S. A. H.). The authors declare that they have no conflicts of interest with the contents of this article. The content is solely the responsibility of the authors and does not necessarily represent the official views of the National Institutes of Health.

This article was selected as one of our Editors' Picks.

[1] Both authors contributed equally to this work.

[2] Present address: Dept. of Systems Biology, Warren Alpert Bldg. 412, 200 Longwood Ave., Harvard Medical School, Boston, MA 02115.

[3] To whom correspondence should be addressed: Dept. of Molecular Biology and Genetics, Cornell University, 245 Biotechnology Bldg., Ithaca, NY 14853. Tel.: 607-254-8717; Fax: 607-255-6249; E-mail: sah42@cornell.edu.

[4] The abbreviations used are: ER, endoplasmic reticulum; TAG, triacylglycerols; PI, phosphatidylinositol; PA, phosphatidic acid; DAG, diacylglycerol; PS, phosphatidylserine; PE, phosphatidylethanolamine; PC, phosphatidylcholine; FFA, free fatty acids; SE, steryl ester; CL, cardiolipin; I, inositol; C, choline; ERMES, ER–mitochondria encounter structure; PCC, Pearson's correlation coefficient; FAM, 6-carboxyfluorescein; TAMRA, tetramethylrhodamine; PCC, Pearson correlation coefficient.

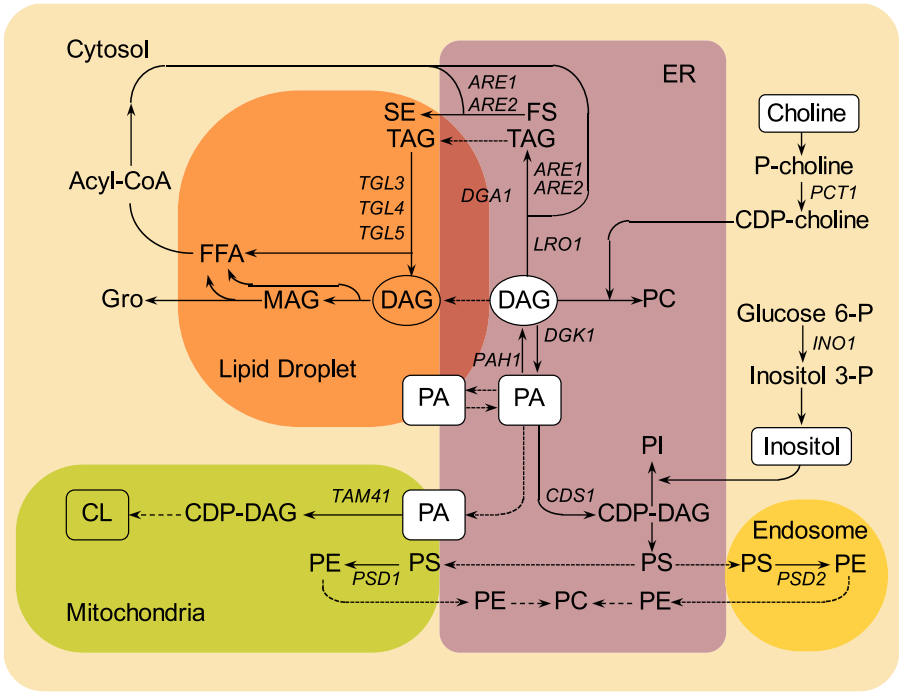

Figure 1. Localization of key lipids and enzymes, designated by the genes encoding them, in different cellular compartments in *S. cerevisiae*. PA serves as precursor to both phospholipids and neutral lipids. PA is found in the ER (*purple box*), in lipid droplets (*orange box*), and in mitochondria (*green box*). In the ER, PA serves as immediate precursor of CDP-DAG, precursor to PI and PS. PS is converted into PE by decarboxylation in the mitochondria or in the endosome compartment (*accented yellow box*). PC is synthesized by methylation of PE or from DAG and CDP-choline. DAG is derived from dephosphorylation of PA or deacylation of TAG. Acyl-CoA is localized in the cytosol (*light yellow box*) and serves as fatty acid pool for the synthesis of PA, TAG, and SE. PA is also transported from the ER to the mitochondria, where it generates CDP-DAG and CL. The positions of PA within the metabolic network are *boxed*, the positions of DAG are *circled*, and the positions at which inositol and choline enter in the metabolic pathway are *boxed*. The *arrows* represent routes of metabolic conversion. The names of the structural genes encoding enzymes catalyzing specific metabolic conversions are shown *adjacent to* the *arrows*.

In addition to elevated levels of PA, retention of Opi1p in the ER also requires its interaction with Scs2p (15). Scs2p, homolog of mammalian synaptobrevin-associated protein (VAMP), is a conserved integral ER protein and a component of a lipid-sensing complex (17–19). Proteins of the VAMP family serve as anchors to the ER for cytoplasmic proteins, including Opi1p, through a conserved motif known as FFAT, two phenylalanines (FF) in an Acidic Tract (19, 20). Many proteins to which VAMP binds are targeted to other intracellular membranes. This implies that VAMP is an important bridge between the ER and a wide variety of organelles at membrane contact sites (21), serving to facilitate lipid transfer and communication between organelles (22–24). For example, in yeast, phosphatidylinositol 4-phosphate levels on the plasma membrane are regulated at membrane contact sites through interaction between Scs2p and Osh3p (25). In addition, deletion of *SCS2* leads to a 50% loss in ER-plasma membrane contact sites (26). However, to date, no role for Opi1p in lipid transfer between ER and other membrane compartments has been reported.

Both *scs2*Δ and *opi1*Δ mutants exhibit complex, pleiotropic phenotypes, related to lipid metabolism and gene regulation (19, 27–30). The yeast *SCS2* gene was originally isolated as a high copy suppressor of choline sensitivity (39), a phenotype associated with an uncharacterized dominant mutation, *CSE1* (31). Scs2p was subsequently identified as an integral membrane protein of the ER (17) and homolog of the mammalian VAMP (32). The *scs2*Δ mutant exhibits a relatively weak Ino$^-$ phenotype at 30 °C, which becomes stronger (more visible in plate tests) at growth temperatures of 34 °C or higher (Fig. 2, *A* and *B*). The *scs2*Δ Ino$^-$ phenotype also becomes more stringent in the presence of exogenous choline (14) (Fig. 2, *A* and *B*) and is suppressed by mutations in the CDP-choline pathway for PC biosynthesis (17, 18). The *opi1*Δ mutation, in contrast, confers constitutive overexpression of *INO1* and other UAS_{INO}-containing genes (3–5, 33), resulting in overproduction and excretion of inositol into the growth medium (Opi$^-$ phenotype). The *opi1*Δ mutant also exhibits a Pet$^-$ phenotype (*i.e.* inability to survive complete loss of the mitochondrial genome) and produces very reduced levels of the mitochondrial lipid, CL (34). CL is synthesized in the inner mitochondrial membrane in a multistep pathway (Fig. 1), using PA synthesized in the ER and transferred to mitochondria via the ER–mitochondria encounter structure (ERMES) (35–38).

A major goal of the current study was to determine which of the diverse regulatory and metabolic phenotypes conferred by the *scs2*Δ and *opi1*Δ mutations result from the loss of the interaction between Opi1p and Scs2p in the ER. Moreover, given the importance of the FFAT motif in facilitating interorganelle lipid transfer (21), we examined the specific function of the interaction of Opi1p and Scs2p in regulation of lipid metabolism. For this purpose, we used the BY4742 parent strain to mutate the FFAT domain in *OPI1*, within its genomic locus, to create an *OPI1*^{ffat} strain. A second goal was to determine the individual and relative roles of inositol and choline on both lipid metabolism and regulation of *INO1*. In each of three congenic strains, BY4742 (wild type), *scs2*Δ (SJY39), and *OPI1*^{ffat}

(YCY47), we also tagged *OPI1* or *OPI1*^{ffat} with GFP within the *OPI1* genomic locus, to analyze and compare the kinetics of changes in lipid metabolism, Opi1p or Opi1^{ffat}p localization, and *INO1* derepression in cells shifted from inositol-containing to inositol-free medium in the presence and/or absence of choline. We report here that the *OPI1*^{ffat} mutant exhibits relatively weak inositol auxotrophy (Ino$^-$ phenotype), which, similar to the phenotype of the *scs2*Δ mutant (14, 17), becomes stronger at higher growth temperatures and in the presence of choline. Moreover, Opi1p in the *scs2*Δ strain and Opi1^{ffat}p in the *OPI1*^{ffat} strains, respectively, did not exit the nucleus following a shift to medium lacking inositol when choline was present, and under these conditions, *INO1* failed to derepress. Thus, we conclude that these phenotypes are conferred by the loss of the Opi1p–Scs2p interaction in the ER. Moreover, we observed that loss of the Opi1p–Scs2p interaction in the ER results in reduced content of the mitochondrial lipid CL under all growth conditions tested, indicating that PA transfer from the ER to the mitochondria is impaired in the absence of this interaction. These results suggest a heretofore unrecognized role for Scs2p–Opi1p interaction in lipid transfer from ER to mitochondria.

Results

The scs2Δ and OPI1^{ffat} mutations confer inositol auxotrophy that is strengthened in the presence of choline and at higher growth temperatures

In this study, we sought to investigate the root cause of the choline-sensitive inositol auxotrophy phenotype of *scs2*Δ. The *scs2*Δ mutant exhibits reduced growth in the absence of inositol (Ino$^-$ phenotype), which is most evident at higher growth temperatures (Fig. 2, *A* and *B*) (18, 19, 40) and in the presence of exogenous choline (14) (Fig. 3). The *scs2*Δ Ino$^-$ phenotype is also suppressed by mutations in the CDP-choline pathway for PC biosynthesis (18), indicating that incorporation of choline into phospholipids via this pathway is involved in the Ino$^-$ phenotype of *scs2*Δ (Fig. 3).

Because a functional FFAT domain is necessary for interaction of Opi1p with Scs2p in the ER, we asked whether an *OPI1*^{ffat} strain exhibits phenotypes similar to those observed in the *scs2*Δ strain. We reasoned that shared phenotypes in these two strains indicate a functional role for this important interaction. To test this hypothesis, we used the BY4742 parent strain to mutate the FFAT domain in *OPI1*, within its genomic locus, thereby creating the *OPI1*^{ffat} strain. The *OPI1*^{ffat} (YCY47) and *scs2*Δ (SJY39) strains were then tested and compared in standard plate assays for their ability to grow in the absence of inositol at 30 and 34 °C in the presence and/or absence of choline. The *OPI1*^{ffat} and *scs2*Δ strains both exhibit similar (weak) inositol auxotrophy at 30 °C. (Compare the stringent Ino$^-$ phenotype of *ino1*Δ with the weak Ino$^-$ phenotypes of *scs2*Δ and *OPI1*^{ffat} at 30 °C; Fig. 2*A*). The Ino$^-$ phenotype of both *scs2*Δ and *OPI1*^{ffat} is strengthened at 34 °C and further enhanced when choline is present at 34 °C (Fig. 2*B*). Because *scs2*Δ and *OPI1*^{ffat} *SCS2* share only one defect in common, namely the lack of a functional Scs2p–Opi1p interaction in the ER, we conclude that loss of this interaction is responsible for these growth

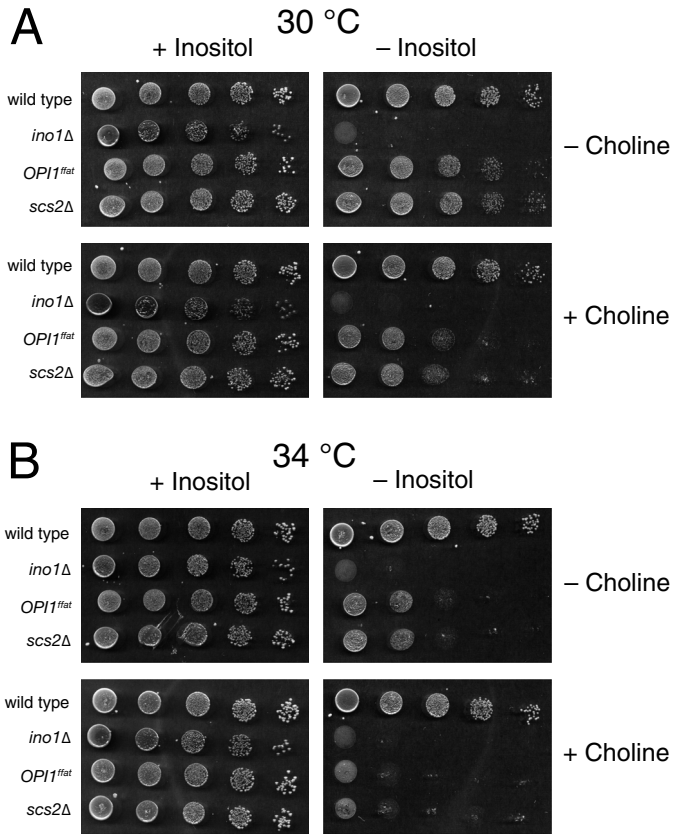

Figure 2. Inositol auxotrophy (Ino$^-$ phenotype) of the *OPI1*^{ffat} and *scs2*Δ mutants at different temperatures. A suspension of BY4742 (wild type), YCY47 (*OPI1*^{ffat}), and SJY39 (*scs2*Δ) cells at a concentration of 1.0 $A_{600\ nm}$/ml and four subsequent 1:10 serial dilutions of strains were spotted on I^+C^-, I^-C^-, I^+C^+, and I^-C^+ plates and allowed to grow for 2 days at 30 °C (*A*) or 34 °C (*B*). SJY425 (*ino1*Δ) serves as a control for the Ino$^-$ phenotype.

phenotypes. Thus, interaction of Opi1p with Scs2p in the ER is required, in addition to its interaction with PA, for optimal growth in the absence of inositol, especially at higher growth temperatures and in the presence of choline.

We also deleted *PCT1*, encoding choline-phosphate cytidylyltransferase (41), in the *OPI1*^{ffat} and *scs2*Δ strains, thereby blocking incorporation of choline via the CDP-choline (Kennedy) pathway for PC synthesis (42) (Fig. 1). The *pct1*Δ mutation suppressed choline-sensitive inositol auxotrophy phenotype in both *OPI1*^{ffat} and *scs2*Δ strains (Fig. 3). Thus, choline has to enter the CDP-choline pathway for PC synthesis to influence the Ino$^-$ phenotype of the *scs2*Δ and *OPI1*^{ffat} strains. PC synthesized in the ER via CDP-choline pathway utilizes diacylglycerol (DAG), which also serves as the immediate precursor to triacylglycerol (TAG), a major constituent of lipid droplets (Fig. 1). In addition, we constructed and tested a diploid strain, *OPI1*^{ffat}/*OPI1*, to determine whether the *OPI1*^{ffat} mutation was dominant or recessive in terms of its growth in the presence and absence of inositol and choline at 30 and 34 °C. The diploid strain, *OPI1*^{ffat}/*OPI1*, exhibited a slight growth reduction on I^-C^- and I^-C^+ medium (data not shown), a phenotype intermediate between that observed in the wild-type and *OPI1*^{ffat} strains, indicating that the *OPI1*^{ffat} mutation is semidominant with respect to its sensitivity to choline in the absence of inositol. This result implies that both gene products are expressed

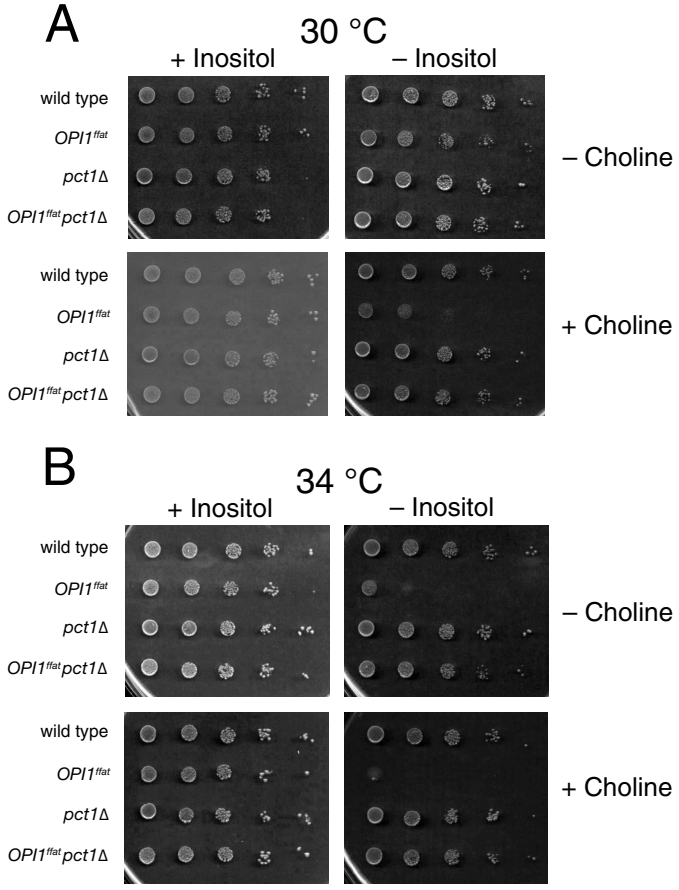

Figure 3. The *pct1*Δ mutation suppresses the Ino$^-$ phenotype of the *OPI1^{ffat}* strain at all temperatures and in the presence of choline. Suspension of BY4742 (wild type), YCY47 (*OPI1^{ffat}*), LGY169 (*pct1*Δ), and LGY541 (*OPI1^{ffat} pct1*Δ) cells at a concentration of 1.0 $A_{600\ nm}$/ml and four subsequent 1:10 serial dilutions of strains were spotted on I^+C^-, I^-C^-, I^+C^+, and I^-C^+ plates and allowed to grow for 2 days at 30 °C (*A*) or 34 °C (*B*).

from the native promoter of *OPI1* and contribute proportionately to the phenotype of the diploid.

*The effects of the OPI1^{ffat} and scs2*Δ *mutations on INO1 expression and Opi1p localization following a shift to inositol-free medium in the absence of choline*

Manipulation of PA levels following withdrawal of inositol and its subsequent readdition in the presence or absence of choline provides a powerful method for analyzing the relative effects of PA on Opi1p function (15, 43). To this end, we analyzed and compared the relative timing of changes in lipid metabolism, Opi1p localization, and *INO1* expression in the wild-type (YCY3), *OPI1^{ffat}* (YCY5), and *scs2*Δ (YCY7) strains under these growth conditions.

As expected, before the shift to inositol-free medium in the absence of choline (*i.e.* from I^+C^- to I^-C^- medium) at 30 °C, *INO1* was fully repressed in the wild-type strain (repressed level set arbitrarily at 1 unit of expression) (Fig. 4*A*). Under these conditions, Opi1p-GFP was localized exclusively to the nucleus (Fig. 4*B*, 0 h, *left panel*). At 1 h following the shift to I^-C^- medium, Opi1p-GFP, in the wild-type strain, had largely exited the nucleus and translocated, primarily to the perinuclear ER region, with a slight residual pool of fluorescence remaining visible within the nucleus (Fig. 4*B*, 1 h, *left panel*). During this

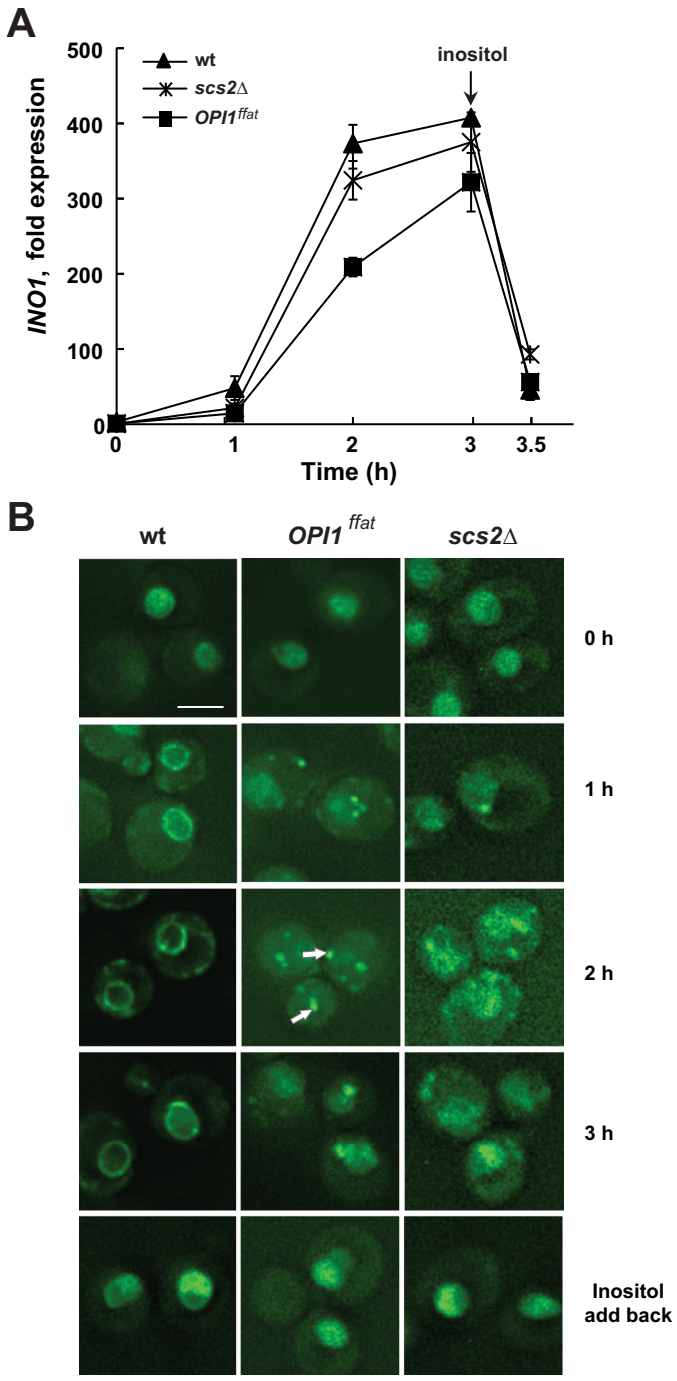

Figure 4. Derepression of the *INO1* gene and localization of Opi1p-GFP in wild type, *OPI1^{ffat}*, and *scs2*Δ strains following a shift to medium lacking inositol and choline. *A*, overnight cultures of YCY3 (wild type), YCY5 (*OPI1^{ffat}*), and YCY7 (*scs2*Δ) expressing genomic Opi1p-GFP were diluted to $A_{600\ nm}$ = 0.2 in I^+C^- medium and allowed to grow to mid-logarithmic phase at 30 °C. Cells were harvested by centrifugation and washed and resuspended in I^- medium, followed by incubation for 3 h at the same temperature. Inositol was added back after 3 h of inositol starvation. Samples were taken at 0, 1, 2, and 3 h of inositol starvation and 30 min after adding back inositol. Total RNA was isolated and analyzed by RT-PCR as described under "Experimental procedures." *Solid triangles*, wild type; *solid squares*, *OPI1^{ffat}*; *solid crosses*, *scs2*Δ. *B*, Opi1p-GFP localization over the same time course. Cells were imaged by fluorescence microscopy. A representative *z*-section is chosen for each image. *Scale bar*, 5 μm. *White arrows*, Opi1p-GFP associated with distinctive puncta.

interval, consistent with the partial exit of Opi1p-GFP from the nucleus (Fig. 4*B*, 1 h, *left panel*), *INO1* expression increased about 50-fold (Fig. 4*A*). Within the interval from 1 to 2 h following the shift to I^-C^- medium, expression of *INO1* increased from 50-fold to about 375-fold in the wild-type strain (Fig. 4*A*). After 2 h in I^-C^- medium, the rate of increase in *INO1* expression leveled off, rising slightly above 410-fold (Fig. 4*A*). At this time point, a significant pool of Opi1p-GFP was still visible in the perinuclear ER region (Fig. 4*B*, 2 h, *left panel*).

In contrast to the relatively rapid initial increase in *INO1* expression in the wild-type strain, *INO1* expression in the *OPI1*^{ffat} and *scs2*Δ strains increased by only about 15-fold during the first hour following the shift to I^-C^- medium (Fig. 4*A*). After the shift to inositol-free medium in the absence of choline (Fig. 4), the nuclear pool of Opi1^{ffat}p-GFP had become less intense by 2 h but was still visible in most cells (Fig. 4*B*, 2 h, *middle panel*). After 2 h in I^-C^- medium, Opi1p^{ffat}-GFP in the *OPI1*^{ffat} strain was associated with distinctive "puncta" (about 3–6/cell), and the nuclear pool of Opi1^{ffat}p-GFP had become less intense but was still visible in most cells (Fig. 4*B*, 2 h, *middle panel*). At this time, *INO1* expression in the *OPI1*^{ffat} strain had increased by 210-fold, still significantly lagging the 375-fold increase seen in wild type (Fig. 4*A*). However, within 3 h following the shift to I^-C^- medium, *INO1* expression in *OPI1*^{ffat} had increased 320-fold, and signal from Opi1^{ffat}p-GFP had reappeared to some extent in the nucleus, with fewer distinctive puncta (1–2/cell) remaining visible (Fig. 4*B*, 3 h, *middle panel*). In the *scs2*Δ strain, Opi1p-GFP fluorescence was still visible in the nucleus at 1 h following the shift to inositol-free medium (Fig. 4*B*, 1 h, *right panel*). At this time, one or two puncta, similar in appearance to those associated with Opi1^{ffat}p-GFP in the *OPI1*^{ffat} strain, were visible adjacent to the nucleus or plasma membrane in the *scs2*Δ strain (Fig. 4*B*). By 2 h following the shift to inositol-free medium, Opi1p-GFP in the *scs2*Δ strain had translocated more prominently to puncta adjacent to nucleus and plasma membrane. However, unlike either wild type or *OPI1*^{ffat} (Fig. 4*B*, 2 h, *left* and *middle panels*), a diffuse pattern of Opi1p-GFP also persisted throughout the cell in the *scs2*Δ strain, possibly reflecting a reduction in cortical ER associated with the *scs2*Δ mutation, as reported by Loewen *et al.* (29). At 3 h, a diffuse pattern of Opi1p-GFP localization also remained visible in the nuclear region in the *scs2*Δ strain.

However, despite differences between the *scs2*Δ and wild-type strains in the pattern of Opi1p-GFP localization (Fig. 4*B*) following the shift to I^-C^- medium, overall expression of *INO1* in the *scs2*Δ strain reached levels only slightly lower than those seen in wild type (Fig. 4*A*). By 2 h following the shift to I^-C^- medium, *INO1* expression had increased by 325-fold in the *scs2*Δ strain, a level close to the 375-fold increase observed in the wild-type control during the same interval. Within 3 h following the shift to I^-C^- medium, *INO1* expression had increased by 375-fold in the *scs2*Δ strain, a level that is not significantly different in comparison with the 410-fold increase observed in the wild-type strain (Fig. 4*A*). In contrast, *INO1* expression in the *OPI1*^{ffat} strain remained somewhat lower in comparison with the other two strains at each time point following the shift to inositol-free medium (Fig. 4*A*). After 3 h following the shift to I^-C^- medium, inositol was added back to each of the cultures. *INO1* expression in all three strains decreased within about 30 min to values similar to those observed in these same strains between 0 and 1 h following the shift from I^+C^- to I^-C^- medium (Fig. 4*A*). Translocation of Opi1-GFP or Opi1^{ffat}p-GFP back into the nuclei of the respective strains was observed within this same 30-min interval (Fig. 4*B*).

The puncta associated with Opi1^{ffat}p-GFP, following a shift to medium lacking both inositol and choline, are ER-bound lipid droplets

As described above, within 2 h following a shift of the *OPI1*^{ffat} strain to I^-C^- medium, a fraction of the fluorescence of Opi1^{ffat}p-GFP was associated with distinctive puncta, adjacent to the perinuclear ER (Fig. 4*B*, 2 h, *middle panel*). In addition to its role as precursor to PI and other membrane forming phospholipids, PA also serves as precursor, via DAG, in the synthesis of TAG (Fig. 1), a major constituent of lipid droplets. The appearance of Opi1^{ffat}p-GFP–associated puncta in cells deprived of inositol is consistent with the report of Han *et al.* (44) showing that Opi1^{ffat}p associates with areas of nascent lipid droplet formation. Therefore, given the morphology of the Opi1^{ffat}p-GFP–labeled puncta and their proximity to the perinuclear ER, we suspected that these puncta represent a pool of PA associated with nascent lipid droplets. To test this hypothesis, we created cells co-expressing Tgl4p-RFP, a lipid droplet marker (45). We observed a significant overlap of Tgl4p-RFP– and Opi1^{ffat}p-GFP–associated puncta following a 2-h shift to I^-C^- medium (Fig. 5*A*, *right*), supporting the identification of the puncta as lipid droplets. After 3 h of inositol starvation, Opi1^{ffat}p-GFP had translocated in part back to the nucleoplasm. Following inositol addition, Opi1^{ffat}p-GFP relocated completely to the nucleus within 30 min (Fig. 4*B*). To further verify and quantify Opi1^{ffat}p co-localization with lipid droplets, we examined the localization of GFP-Opi1^{ffat}p, expressed from a centromeric plasmid, in cells also expressing Erg6p-RFP, a protein that is abundant in yeast lipid droplets (46, 47). Co-localization of Erg6p and Opi1p was quantified using Pearson's correlation coefficient (PCC) (48) in 30 cells that exhibited clear expression of the plasmid versions of GFP-Opi1p or GFP-Opi1^{ffat}p. The co-localization of GFP-Opi1p and RFP-Egr6p, both before and 2 h after the shift from I^+C^- to I^-C^- medium, was not significant (PCC = 0.24 and 0.21, respectively) (Fig. 5*B*). In contrast, in the strain co-expressing GFP-Opi1^{ffat}p and RFP-Erg6p, PCC was 0.27 before the shift and 0.61 by 2 h following the shift to I^-C^- medium (Fig. 5*B*), indicating a significant increase in Opi1^{ffat}p co-localization with lipid droplets at 2 h following the shift to I^-C^- medium. These observations are consistent with previous studies indicating that a pool of PA in the ER and/or lipid droplets (49), used for synthesis of DAG, precursor to TAG (Fig. 1), competes with the pool of PA used in the synthesis of CDP-DAG, precursor to PI and other membrane phospholipids. Thus, in cells grown in the presence of inositol, increased PI synthesis is correlated with decreased TAG accumulation (4, 43, 50, 51).

To further test this hypothesis, translocation of Opi1p-GFP and Opi1^{ffat}p-GFP was also examined in a *dga1*Δ *lro1*Δ *are1*Δ *are2*Δ quadruple mutant (Table 1), which is unable to make

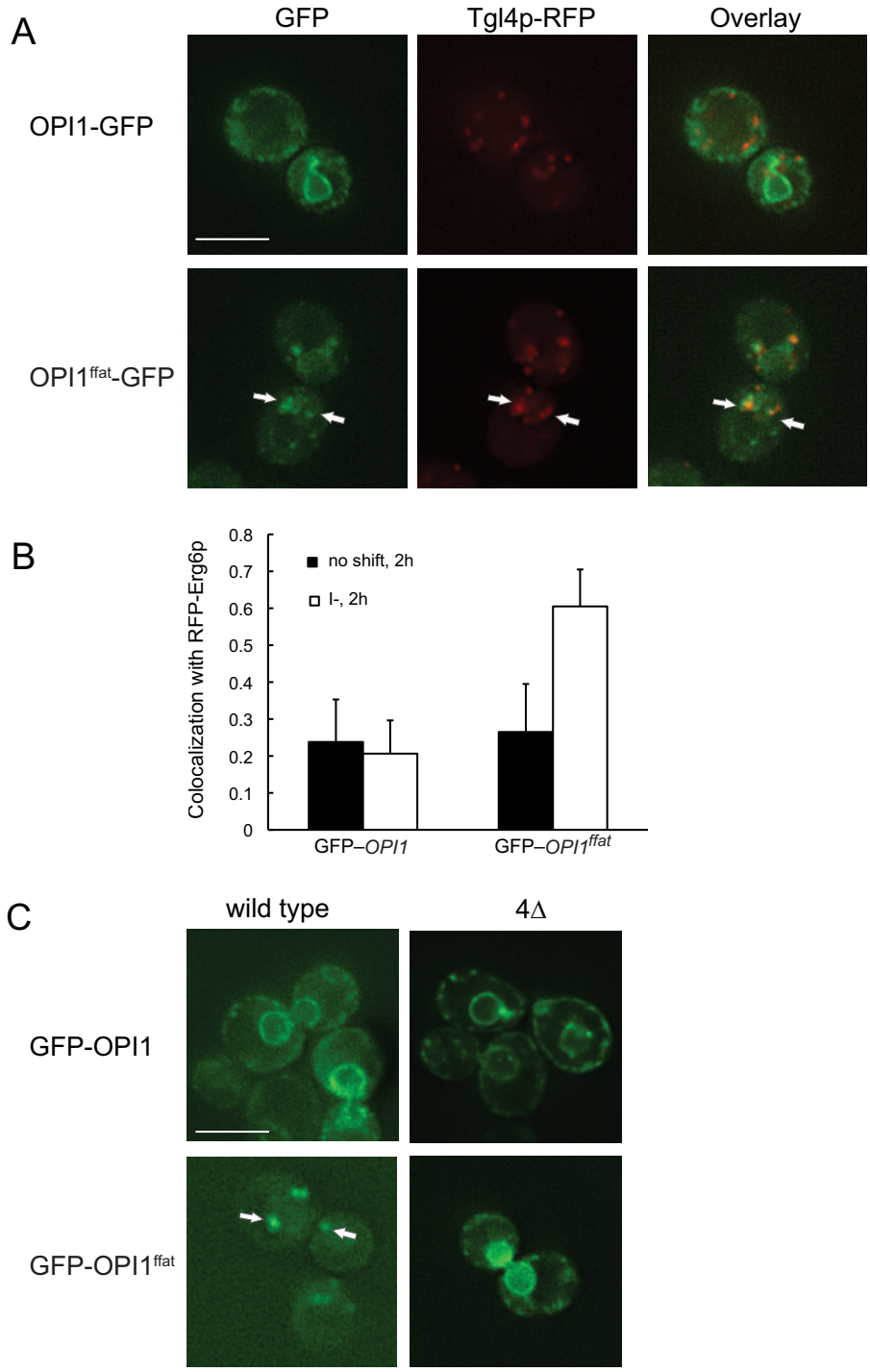

Figure 5. Opi1p^{ffat}-GFP transiently colocalizes with lipid droplets following a shift to medium lacking inositol and choline. Overnight cultures grown in I^+C^- medium at 30 °C were diluted to $A_{600\,nm}$ = 0.2 and allowed to grow to mid-logarithmic phase in I^+C^- medium at 30 °C. Cells were harvested by centrifugation, washed and resuspended in I^-C^- medium, incubated for 2 h, and analyzed by fluorescence microscopy. *A*, Tgl4-RFP, carried on a plasmid, was co-expressed with genomic Opi1p-GFP in wild type (*top*), or with genomic Opi1p^{ffat}-GFP in *OPI1^{ffat}* (*bottom*). *B*, the CMY564 strain expressing genomic RFP-Erg6p was transformed with plasmids expressing either GFP-Opi1p or GFP-Opi1p^{ffat}. Colocalization of Tgl4-RFP with genomic Opi1p-GFP or Opi1p^{ffat}-GFP, respectively, was assessed using PCC (n = 30) between wavelength 528 nm (GFP) and 617 nm (RFP). PCC > 0.5 indicates significant correlation. *C*, the wild-type and *dga1*Δ*lro1*Δ*are1*Δ*are2*Δ quadruple mutant (4Δ) strains were transformed with plasmids expressing either GFP-Opi1p (*top*) or GFP-Opi1p^{ffat} (*bottom*). Cells were grown and collected as indicated above and analyzed by fluorescence microscopy. A representative *z*-section was chosen for each image. *Scale bars*, 5 μm. *Error bars*, S.D.

lipid droplets (52). A plasmid version of GFP-Opi1p or GFP-Opi1^{ffat}p (as described under "Experimental procedures"; see Table 2) was transformed into the wild-type strain and the quadruple mutant. In both strains, GFP-Opi1p translocated to ER membranes within 2 h following transfer to I^-C^- medium (Fig. 5*C*, *top*), following a pattern and kinetics similar to that observed using the genomic Opi1p-GFP construct (Fig. 4*B*, 2 h, *left panel*). Following the shift of the *OPI1^{ffat}* strain expressing

Table 1
Yeast strains used

Strain	Genotype/description	Source/reference
BY4742 (parent strain)	MATα *his3Δ1 leu2Δ0 lys2Δ0 ura3Δ0* (S288C)	Ref. 67
YCY47	BY4742 *OPI1^{ffat}*	This study
SJY39	BY4742 *scs2Δ::KanMX6*	This study
SJY425	BY4742 *ino1Δ::HIS3*	This study
YCY3	BY4742 *OPI1* GFP::*KanMX6*	This study
YCY5	BY4742 *OPI1^{ffat}* GFP::*KanMX6*	This study
YCY7	BY4742 *OPI1* GFP::*KanMX6 scs2Δ::URA3*	This study
LGY169	BY4742 *pct1Δ::LEU2*	This study
LGY541	BY4742 *OPI1^{ffat} pct1Δ::LEU2*	This study
YCY45	BY4742 with pBP73-C[GFP-*OPI1*]	This study
YCY46	BY4742 with pBP73-C[GFP-*OPI1^{ffat}*]	This study
YJP1078	BY4742 *dga1Δ::KanMX4 lro1Δ::KanMX4 are1Δ::KanMX4 are2Δ::KanMX4*	Ref. 71
YCY36	YJP1078 with pBP73-C[GFP-*OPI1*]	This study
YCY37	YJP1078 with pBP73-C[GFP-*OPI1^{ffat}*]	This study
CMY564	BY4742 RFP-ERG6::*KanMX*	Ref. 47
YCY96	CMY564 with pBP73-C[GFP-*OPI1*]	This study
YCY97	CMY564 with pBP73-C[GFP-*OPI1^{ffat}*]	This study

Table 2
Plasmids used

Plasmid	Genotype/description	Source/reference
pFA6a-GFP(S65T)-kanMX	Kanamycin resistance cassette for genomic N terminus tagging of GFP	Ref. 69
pCRCU[*TGL4*-RFP]	*URA3* cassette with *TGL4* cloned at NotI-ClaI	Gift of S. Kohlwein
pBP73-C	pRS416 with the *CPY1* promotor cloned at SacI-XbaI and GFP at Xba-BamHI	Ref. 72
pBP73-C[GFP-*OPI1*]	pBP73-C with *OPI1* cloned at BamHI-HindIII	This study
pBP73-C[GFP-*OPI1^{ffat}*]	pBP73-C with *OPI1^{ffat}* cloned at BamHI-HindIII	This study

the plasmid-borne GFP-Opi1^{ffat}p to I^-C^- medium, fluorescence was also associated with puncta. However, in the *dga1Δlro1Δare1Δare2Δ* strain, Opi1^{ffat}p was mainly localized in the nucleus and the perinuclear region, and no puncta were observed by 2 h following the shift to I^-C^- medium (Fig. 5*C*, *bottom right*), indicating that formation of the puncta is most likely related to lipid droplet formation.

Following a shift to inositol-free medium in the presence of choline, INO1 fails to derepress in the OPI1^{ffat} and scs2Δ strains

In wild-type cells grown in medium containing both inositol and choline and shifted to medium lacking inositol but containing choline (*i.e.* a shift from I^+C^+ to I^-C^+ medium; Fig. 6), derepression of *INO1* was delayed by about 30–60 min in comparison with the same cells shifted to inositol-free medium in the absence of choline (*i.e.* from I^+C^- to I^-C^- medium; Fig. 4*A*). Within 2 h following the shift from I^+C^+ to I^-C^+ medium, Opi1p-GFP in the wild-type strain had exited the nucleus and was distinctly observed in the perinuclear ER (Fig. 6*B*). At this time point, *INO1* expression had increased by about 100-fold (Fig. 4*A*), and by 3 h *INO1* expression had increased by about 400-fold (Fig. 6*A*), an increase comparable with that seen in this same strain after the shift from I^+C^- to I^-C^- for 3 h (Fig. 4*A*).

In marked contrast to the behavior of Opi1p-GFP in the wild-type strain, Opi1^{ffat}p-GFP in the *OPI1^{ffat}* strain completely failed to exit the nucleus following a shift to inositol-free medium in the presence of choline (*i.e.* from I^+C^+ to I^-C^+ medium; Fig. 6*B*). Significantly, the Opi1^{ffat}p-GFP–labeled puncta, observed in association with lipid droplets following the shift of *OPI1^{ffat}* from I^+C^- to I^-C^- medium (Fig. 4*B*, 2 h, *middle panel*), were not observed after the shift from I^+C^+ to I^-C^+ medium (Fig. 6*B*). Similar to Opi1^{ffat}p-GFP in the *OPI1^{ffat}* strain, Opi1p-GFP in *scs2Δ* also failed to exit the nucleus following the shift from I^+C^+ to I^-C^+ medium. Moreover, the Opi1p-GFP–associated puncta, seen in this strain after the shift from I^+C^- to I^-C^- medium, were also not observed (data not shown). Furthermore, *INO1* failed to derepress in both the *OPI1^{ffat}* and *scs2Δ* strains following the shift to I^-C^+ medium (Fig. 6*A*). These observations suggest that a pool of PA, associated with the synthesis of DAG, precursor to TAG in nascent lipid droplets (44), is sufficient to attract Opi1^{ffat}p or Opi1p from the nuclei of the *OPI1^{ffat}* and *scs2Δ* strains, respectively, in the absence of inositol, but only when choline is also absent (compare Fig. 4*B* with Fig. 6*B*). This result is consistent with the hypothesis that synthesis of PC via the CDP-choline pathway (Fig. 1) competes for a pool of DAG derived from PA in the ER, a pool that, in the absence of exogenous choline, is available for increased production of TAG (Fig. 1) and lipid droplet formation (Fig. 4*B*).

Overall cellular PA levels increase in all three strains following a shift from I^+ medium to I^- medium, whether choline is present or not, but do not correlate with INO1 expression in the OPI1^{ffat} and scs2Δ strains when choline is present

To determine whether the lack of the FFAT domain in Opi1p affects PA content, we performed lipid analysis under all growth conditions described above. PA levels in the wild-type strain increased in a comparable fashion following a shift from I^+ to I^- medium, whether choline was present or not (Fig. 7, compare *A* with *B* and *C* with *D*). There was also no significant difference in the levels of PA in the wild-type strain growing in I^+C^- medium *versus* I^+C^+ medium (Fig. 7, compare *A* with *C*). After the shift to inositol-free medium in the absence or presence of choline (*i.e.* from I^+C^- to I^-C^- medium or from I^+C^+ to I^-C^+ medium), PA levels rose significantly in the wild-type strain. However, the kinetics of the increase in PA levels were somewhat affected by the presence of choline, initially spiking

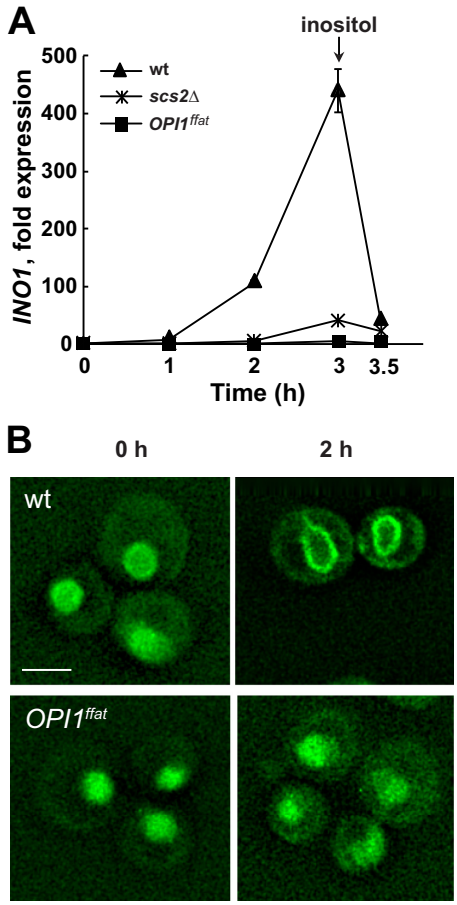

Figure 6. INO1 expression in wild-type, *OPI1*^{ffat}, and *scs2*Δ strains and localization of Opi1p-GFP in wild-type or Opi1^{ffat}p-GFP in *scs2*Δ and *OPI1*^{ffat} strains, respectively, after a shift to I$^-$C$^+$ medium. *A*, overnight cultures of YCY3 (wild type), YCY5 (*OPI1*^{ffat}), and YCY7 (*scs2*Δ) expressing genomic Opi1p-GFP or Opi1p^{ffat}-GFP, respectively, were diluted to A_{600} = 0.2 in I$^+$C$^+$ medium and allowed to grow to mid-logarithmic phase at 30 °C. Cells were harvested by centrifugation, washed and resuspended in I$^-$C$^+$ medium, and incubated for 3 h. Inositol was added back after 3 h of inositol starvation. Samples were taken at 0, 1, 2, and 3 h of inositol starvation and 30 min after adding back inositol. Total RNA was isolated and analyzed by RT-PCR as described under "Experimental procedures." *Solid triangles*, wild type; *solid squares*, *OPI1*^{ffat}; *solid crosses*, *scs2*Δ. *B*, Opi1p-GFP localization in wild type and Opi1p^{ffat}-GFP in *OPI1*^{ffat} at 0 and 2 h after a shift to I$^-$C$^+$ medium. Cells were imaged by fluorescence microscopy. A representative *z*-section was chosen for each image. *Scale bar*, 5 μm.

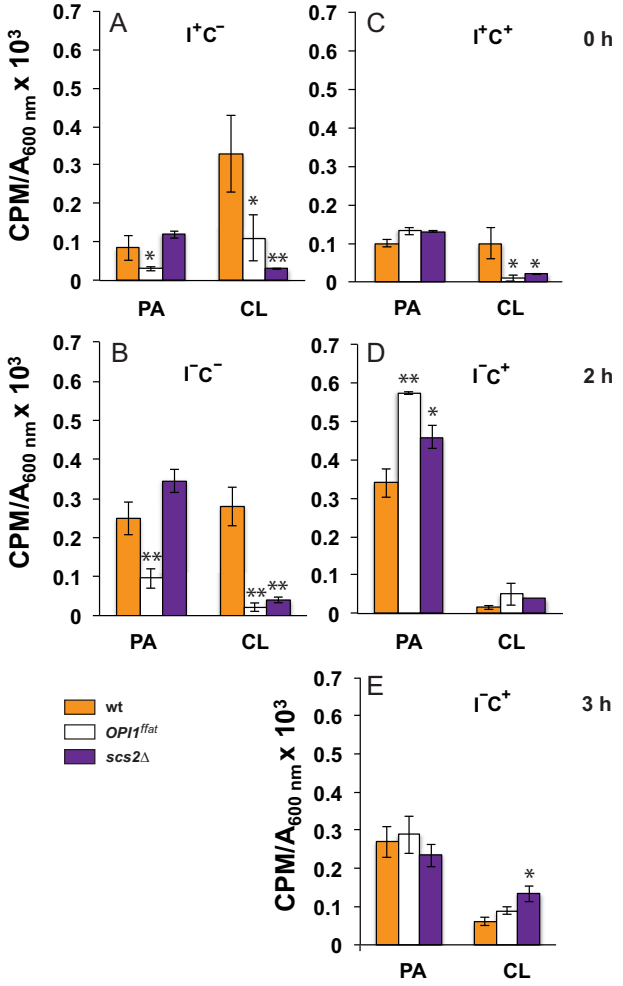

Figure 7. PA and CL levels in wild-type and mutant strains following a shift to medium lacking inositol. Overnight cultures grown in I$^+$C$^-$ or I$^+$C$^+$ medium at 30 °C in the presence of ^{32}P as described under "Experimental procedures" were diluted to $A_{600\ nm}$ = 0.2 in I$^+$C$^-$ or I$^+$C$^+$ medium at 30 °C maintaining label constant. Cells were allowed to grow to mid-logarithmic phase, and samples (time 0) were collected for lipid analysis (*A* and *C*). The remaining cultures were filtered and resuspended in I$^-$C$^-$ medium or I$^-$C$^+$ medium maintaining label constant. Cultures growing in I$^-$C$^-$ were allowed to continue growing for an additional 2 h (*B*), whereas I$^-$C$^+$ cultures were allowed to grow for an additional 2 and 3 h (*D* and *E*, respectively). At these time points, cells were collected for lipid analysis. Data are expressed as cpm of radiolabel ^{32}P incorporated into total phospholipids per OD unit in the cell culture. Data are expressed as mean ± S.D. (*error bars*) (n = 3). **, $p < 0.005$; *, $p < 0.05$.

higher at 2 h following the shift to I$^-$C$^+$ (Fig. 7*D*) and then dropping down by 3 h (Fig. 7*E*) to a level comparable with that seen at 2 h after the shift to I$^-$C$^-$ medium (Fig. 7*B*). At 2 h after the shift to I$^-$C$^+$ medium, *INO1* expression in wild type was significantly lower (Fig. 6*A*) than the level seen by 2 h following the shift to I$^-$C$^-$ medium (Fig. 4*A*). However, by 3 h following the shift to I$^-$C$^+$ medium (Fig. 6*A*), *INO1* expression in wild type had reached levels as high as or higher than those observed in this strain after the shift to I$^-$C$^-$ medium (Fig. 4). This transient contrast between the kinetics of rising PA levels and *INO1* derepression, in the presence *versus* the absence of choline, suggests that the rising pool of PA, accompanying the removal of inositol, is not as rapidly available for interaction with Opi1p as it is when choline is absent, an issue to be taken up under "Discussion."

In contrast to both the wild-type and *scs2*Δ strains, PA levels in the *OPI1*^{ffat} strain were significantly lower when growing in medium lacking choline, whether inositol was present or not (compare PA levels in *OPI1*^{ffat} in comparison with wild type and *scs2*Δ; Fig. 7, *A* and *B*). This observation is consistent with the somewhat reduced level of *INO1* expression observed in this strain in comparison with wild type after the shift to I$^-$C$^-$ medium (Fig. 4*A*). Nevertheless, in each of the three strains, PA levels increased about 2-fold following the shift from I$^+$C$^-$ medium to I$^-$C$^-$ medium (Fig. 7). Furthermore, in each of the three strains, in the absence of choline, the increase in PA that followed the shift from I$^+$C$^-$ to I$^-$C$^-$ medium was correlated with the exit of Opi1p-GFP or Opi1p^{ffat}-GFP, respectively, from the nucleus (Fig. 4*B*) and with derepression of *INO1* (Fig. 4*A*). Strikingly, however, after a shift to inositol-free medium in the presence of choline, Opi1p-GFP and Opi1p^{ffat}-GFP in the *OPI1*^{ffat} and *scs2*Δ strains, respectively, failed to exit the nucleus, and *INO1* failed to derepress (Fig. 6). Significantly,

the failure of *INO1* derepression in these two strains under these conditions occurred despite rising PA levels, comparable with or higher than those observed in the wild-type strain after the shift to I^-C^+ medium (compare PA levels in all three strains; Fig. 7, *B*, *D*, and *E*). Thus, when choline is present, direct interaction of Opi1p and Scs2p in the ER, in addition to rising cellular PA levels, is essential for *INO1* expression.

CL levels are significantly reduced in the OPI1^{ffat} and scs2Δ strains

In yeast, PA serves as precursor to two separate pools of CDP-DAG. In the ER, Cds1p catalyzes the production of CDP-DAG used in the synthesis of PI and PS (Fig. 1). PA used in the synthesis of CDP-DAG in the inner mitochondrial membrane is synthesized in the ER and must be transferred to the outer mitochondrial membrane (53–55) (Fig. 1), primarily via the ERMES (35–38). From the outer mitochondrial membrane, PA must be transferred to the inner mitochondrial membrane by a process requiring the Ups1p–Mdm35 complex (36, 53, 56). Once transferred to the inner mitochondrial membrane, PA serves as precursor to CDP-DAG, catalyzed by the mitochondrial CDP-DAG synthase, Tam41p (Fig. 1) (54). CDP-DAG is then converted to phosphatidylglycerol phosphate in the mitochondria. Phosphatidylglycerol phosphate is then dephosphorylated to form phosphatidylglycerol, the immediate precursor of CL (54).

Despite the significant increase in the wild-type strain in the level of PA, CL content was not greatly affected by the shift from I^+C^- to I^-C^- medium (in Fig. 7, compare relative changes in PA and CL levels in *A* with those in *B*). Moreover, in comparison with wild type, PA levels in the *OPI1^{ffat}* strain were somewhat reduced, whereas those in *scs2*Δ were elevated, both before and after the shift to I^-C^- medium (Fig. 7, *A* and *B*). However, CL levels were greatly reduced in both *OPI1^{ffat}* and *scs2*Δ, in comparison with wild type, both before and after the shift from I^+C^- to I^-C^- medium (Fig. 7, compare data in *A* with data in *B*). Because low CL content was reported in the *opi1*Δ strain in combination with a Pet^- phenotype (34), we assessed growth of the *scs2*Δ and *OPI1^{ffat}* strains, in comparison with wild type, on YPD plates supplemented with ethidium bromide, for the Pet^- phenotype. Growth of all three strains was comparable under these conditions (data not shown). Thus, basic mitochondrial function was not compromised by the changes in lipid metabolism observed in *scs2*Δ and *OPI1^{ffat}* strains. Consistent with these observations, the *scs2*Δ mutant was not identified among the mutations conferring the Pet^- phenotype in a genome-wide screen conducted by Dunn *et al.* (57).

Whereas the shift of the wild-type strain from I^+C^- to I^-C^- medium had little impact on CL levels (Fig. 7, compare *A* with *B*), the presence of choline together with inositol (*i.e.* I^+C^+ *versus* I^+C^- medium) resulted in a significant decrease in CL in comparison with inositol alone (Fig. 7, compare CL levels in wild type in *A* with those in *C*). However, CL levels in the *OPI1^{ffat}* and *scs2*Δ strains were significantly lower than those seen in the wild-type strain under these same conditions (*i.e.* in I^+C^+ medium; Fig. 7*C*). Following the shift from I^+C^+ to I^-C^+ medium, CL level in wild type decreased by an additional 3-fold in the first 2 h (Fig. 7, compare *C* with *D*) but recovered somewhat during the interval from 2 to 3 h (Fig. 7*E*). As described above, in contrast, the level of PA, precursor to CL, increased significantly in the wild-type strain after the shift from I^+C^+ to I^-C^+ medium (Fig. 7, compare *C* with *D* and *E*). Thus, the continuing low level of CL after the shift to I^-C^+ medium suggests that a specific pool of PA, accessible for transport from the ER to mitochondria in wild-type cells, is specifically impacted in the presence of exogenous choline.

TAG levels increased in all three strains after a shift to inositol-free medium in the absence of choline; however, when inositol and choline were both present, neutral lipid composition was affected in distinctly different ways in each of the three strains

TAG levels rose significantly in all three strains after the shift to inositol-free medium in the absence of choline (*i.e.* I^+C^- medium to I^-C^- medium; Fig. 8, compare *A* with *B*). However, DAG, the immediate precursor of TAG (Fig. 1), showed relatively little change in any of the three strains following a shift from I^+C^- medium to I^-C^- medium (Fig. 8, compare DAG levels in *A* with those in *B*). Indeed, in the wild-type strain, shifting from I^+C^- medium to I^-C^- medium had relatively little effect on any single neutral lipid category other than TAG (Fig. 8, *A* and *B*), as reported previously (43, 50). In contrast, in the *OPI1^{ffat}* and *scs2*Δ strains, free fatty acids (FFA) were reduced, in comparison with wild type, both before and after the shift from I^+C^- medium to I^-C^- medium, and steryl ester (SE) levels in these two strains were reduced only after the shift to I^-C^- medium. Free sterols were also significantly reduced in the *OPI1^{ffat} SCS2* strain in comparison with *OPI1 SCS2* both before and after the shift from I^+C^- medium to I^-C^- medium (Fig. 8, compare *A* with *B*).

However, in the presence of both choline and inositol (I^+C^+ medium; Fig. 8*C*), as compared with inositol alone (I^+C^- medium; Fig. 8*A*), the wild-type strain exhibited reductions of 50% or more in essentially all neutral lipids. In stark contrast to wild type, in the *scs2*Δ strain, every category of neutral lipid, except free sterols, was elevated in I^+C^+ medium (Fig. 8*C*), as compared with I^+C^- medium (Fig. 8*A*). In the *OPI1^{ffat}* strain, the levels of essentially all of the individual neutral lipids growing in I^+C^+ medium were intermediate between the other two strains. However, neutral lipid levels in the *OPI1^{ffat}* strain were more similar to those seen in wild type than in *scs2*Δ. We conclude that the higher levels of FFA, TAG, and SE observed in the *scs2*Δ strain growing in I^+C^+ medium are attributable to functions of Scs2p beyond its interaction with Opi1p in the ER.

After the shift to inositol-free medium in the presence of choline (*i.e.* from I^+C^+ to I^-C^+ medium), essentially all categories of neutral lipids in the wild-type strain increased (Fig. 8, compare *C* with *D*) while remaining generally lower, especially with respect to TAG, SE, and FFA, than the levels seen in this same strain after the shift from I^+C^- medium to I^-C^- medium (Fig. 8, compare data in *B* with data in *D*). However, DAG, immediate precursor to both PC via the CDP-choline pathway and TAG, a major constituent of lipid droplets (Fig. 1), is an exception. DAG levels were significantly lower in the wild-type strain growing in I^+C^+ *versus* I^+C^- medium (Fig. 8, compare *A* with *C*) but increased about 2-fold after the shift from I^+C^+ to

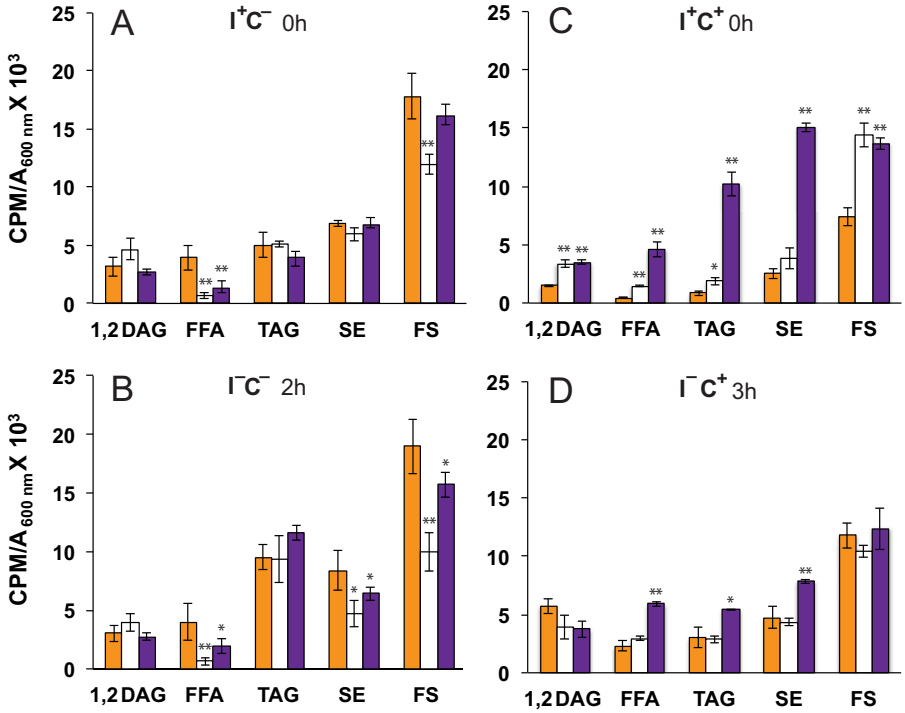

Figure 8. Neutral lipid levels in wild-type and mutant strains following a shift to medium lacking inositol. *A–D*, analysis of neutral lipid classes of YCY3 (wild type), YCY5 (*OPI1*^{ffat}), and YCY7 (*scs2*Δ) strains grown in the presence of [1-^{14}C]acetate in the same conditions described in the legend to Fig. 7. Data are expressed as cpm of radiolabel 1-^{14}C incorporated into neutral lipids per OD unit in the cell culture. Data are expressed as mean ± S.D. (*error bars*) ($n = 3$). **, $p < 0.005$; *, $p < 0.05$.

I^-C^+ medium (compare data in Fig. 8, *C* and *D*). In contrast, no significant change in DAG levels occurred in the wild-type strain following the shift to inositol-free medium in the absence of choline (*i.e.* from I^+C^- to I^-C^- medium; Fig. 8, compare data in *A* with data in *B*). DAG levels in the *OPI1*^{ffat} and *scs2*Δ strains, which were higher in I^+C^+ medium than those seen in wild type, also did not change significantly after the shift from to I^-C^+ medium.

However, following the shift from I^+C^+ to I^-C^+ medium, both TAG and SE levels underwent significant reductions in the *scs2*Δ strain, changes that were far more dramatic than those observed in *OPI1*^{ffat} or wild type (Fig. 8, compare data in *C* with data in *D*). The level of FFA was also significantly elevated in *scs2*Δ, in comparison with the other two strains, both before and after the shift from I^+C^+ to I^-C^+ medium (Fig. 8, compare data in *C* with data in *D*). Again, these changes are presumably attributable to functions of Scs2p beyond those controlled by its interaction with Opi1p in the ER.

Effects of inositol and choline on phospholipid composition

Under steady-state growth conditions in the presence of inositol and absence of choline (I^+C^- medium), all three strains exhibited comparable levels of CDP-DAG, PS, and PE (Fig. 9*A*). PI and PC levels were also comparable in the wild-type and *OPI1*^{ffat} strains in I^+C^- medium. However, in the *scs2*Δ strain, PI and PC levels were about 20 and 30% lower, respectively, in comparison with the levels observed in the other two strains (Fig. 9*A*). Following the shift to inositol-free medium in the absence of choline (I^+C^- to I^-C^- medium), levels of PI in all three strains declined significantly, as reported previously for wild-type strains (50), reaching levels equivalent to about 20% of the PI level seen in the wild-type strain before the shift to I^-C^- medium (Fig. 9*B*). The level of PS, precursor to PE (Fig. 1), was comparable in all three strains in I^+C^- medium and increased slightly in all three strains after the shift to I^-C^- medium (Fig. 9, compare data in *A* with data in *B*). However, a significant reduction in PE content was observed in all three strains when growing in the presence of choline, independent of inositol supplementation (compare PE levels in cells grown in the absence of choline (Fig. 9, *A* and *B*) with levels in cells grown in its presence (Fig. 9, *C–E*)) PE is synthesized from PS via two distinct pathways, localized to different cellular compartments, catalyzed either by Psd2p in the endosome or by Psd1p in the mitochondria (58) (Fig. 1). The Psd1p protein precursor is synthesized on cytoplasmic ribosomes and is processed in the mitochondria (59). Transcription of *PSD1* is regulated by the Ino4p, Ino2p, and Opi1p transcription factors in response to inositol availability, whereas *PSD2* is not (7).

The level of PC increased significantly in the wild-type strain (Fig. 9, *A* and *B*) when shifted to inositol-free medium in the absence of choline (*i.e.* from I^+C^- to I^-C^- medium), consistent with previous studies (50). However, when shifted to inositol-free medium in the presence of choline (*i.e.* from I^+C^+ to I^-C^+ medium; Fig. 9, compare data in *C* with data in *D* and *E*), PC levels in wild type changed minimally if at all. PC levels were significantly lower in the *scs2*Δ strain than in the other two strains, both before and after the shift to I^-C^- medium (Fig. 9, *A* and *B*). However, PC in the *scs2*Δ strain, when growing in I^+C^+ medium, was also significantly higher than in I^+C^- medium and was comparable with the level observed in the wild-type strain growing in I^+C^+ medium (Fig. 9*A*).

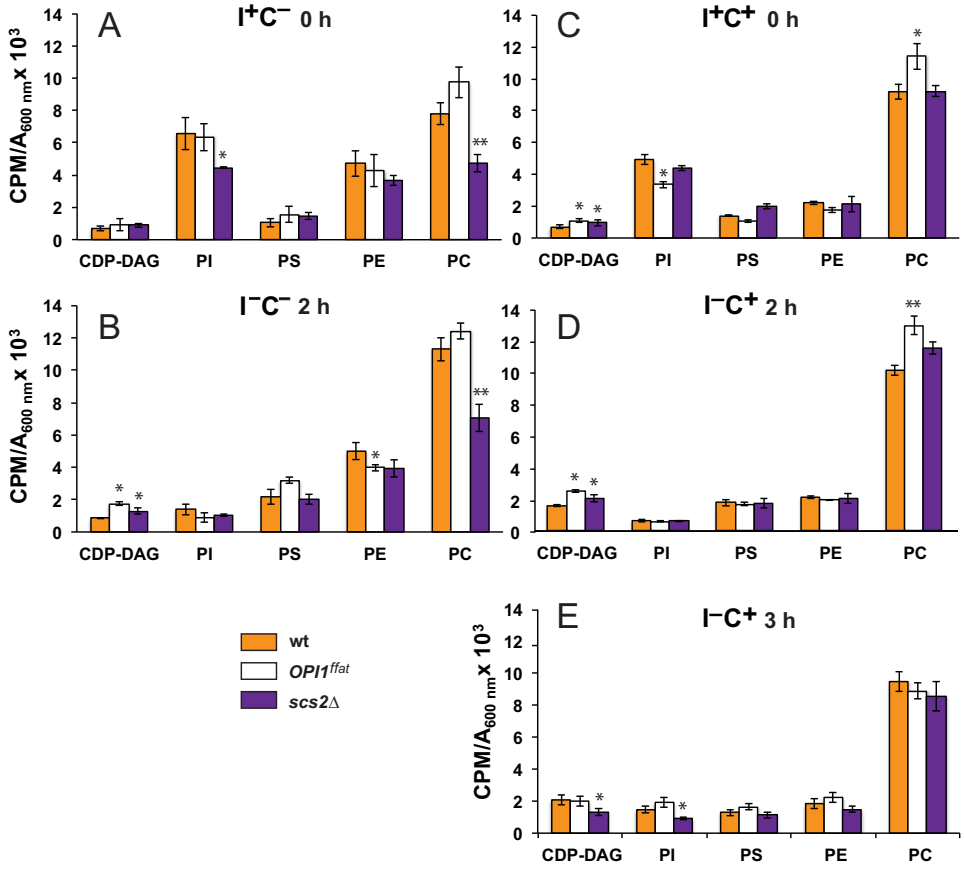

Figure 9. CDP-DAG, PI, PS, PE, and PC levels in wild-type and mutant strains following a shift to medium lacking inositol. YCY3 (wild type), YCY5 (*OPI1*^{ffat}), and YCY7 (*scs2*Δ) strains were grown in the presence of ^{32}P in the same conditions described in the legend to Fig. 7. CDP-DAG, PI, PS, PE, and PC levels are expressed as cpm of radiolabel ^{32}P incorporated into total phospholipids per OD unit in the cell culture. The legend for strains is the same as in Figs. 7 and 8. Data are expressed as mean ± S.D. (*error bars*) ($n = 3$). **, $p < 0.005$; *, $p < 0.05$.

Discussion

In the present study, we compared changes in lipid metabolism and gene regulation in the wild-type, *scs2*Δ, and *OPI1*^{ffat} strains to determine the individual and combined effects of exogenous inositol and choline on lipid metabolism, Opi1p localization, and *INO1* expression. Fig. 10 provides a visual summary of the major findings and the significance of this work. One striking outcome of this study was the discovery that the mitochondrial lipid, CL, is significantly reduced in the *OPI1*^{ffat} and *scs2*Δ strains in comparison with the wild-type strain (Fig. 7). These observations, coupled with the earlier report by Luévano-Martinez *et al.* (34) that the *opi1*Δ mutant exhibits similarly low CL levels, indicate that the reductions in CL content in these strains are most likely due to the loss of the Opi1p–Scs2p interaction in the ER, the one interaction these two proteins share in common. Moreover, we report that the *scs2*Δ and *OPI1*^{ffat} mutations both confer weak Ino$^-$ phenotypes at 30 °C, phenotypes that are strengthened at higher growth temperatures and in the presence of choline (Fig. 2). In contrast, the *opi1*Δ mutant exhibits unregulated high-level constitutive expression of *INO1* and other UAS_{INO}-containing genes and excretes excess inositol into the growth medium (4, 33, 60). Thus, the *opi1*Δ mutant shares no reported metabolic or regulatory phenotype with *scs2*Δ other than low CL levels. To support CL biosynthesis, PA synthesized in the ER must be transferred to the outer mitochondrial membrane and transferred to the inner mitochondrial membrane to be converted to CDP-DAG by Tam41p, the mitochondrial CDP-DAG synthase (35, 53, 54) (Fig. 1). Optimal synthesis of CL requires transfer of PA from the ER to the outer mitochondrial membrane via the ERMES complex (38). The mitochondrial pathway for PE synthesis, similarly, requires the transit of PS from the ER to the mitochondria (55), and deletion of several genes encoding ERMES subunits results in reduced levels of both CL and PE (38). For example, deletion of the *MMM1* gene, encoding an ERMES subunit, containing a conserved "synaptotagmin-like mitochondrial lipid-binding" (SMP) domain (61), is associated with significantly reduced levels of both CL and PE in the mitochondria (38). However, deletion of *MDM34*, encoding an outer mitochondrial membrane protein, is associated with reduced levels of CL but does not affect PE levels (38).

The reductions in CL content that we observed in *scs2*Δ and *OPI1*^{ffat} strains relative to wild type (Fig. 7) are proportionately comparable with the reductions in CL reported in the mitochondrial lipids of mutants carrying deletions of ERMES subunits (38). Thus, the reductions in CL synthesis that we observed in the *scs2*Δ and *OPI1*^{ffat} strains are consistent with the hypothesis that the interaction of Opi1p with Scs2p facilitates transfer of PA from the ER to the mitochondria. Moreover, simultaneous disruption of both ERMES and vCLAMP

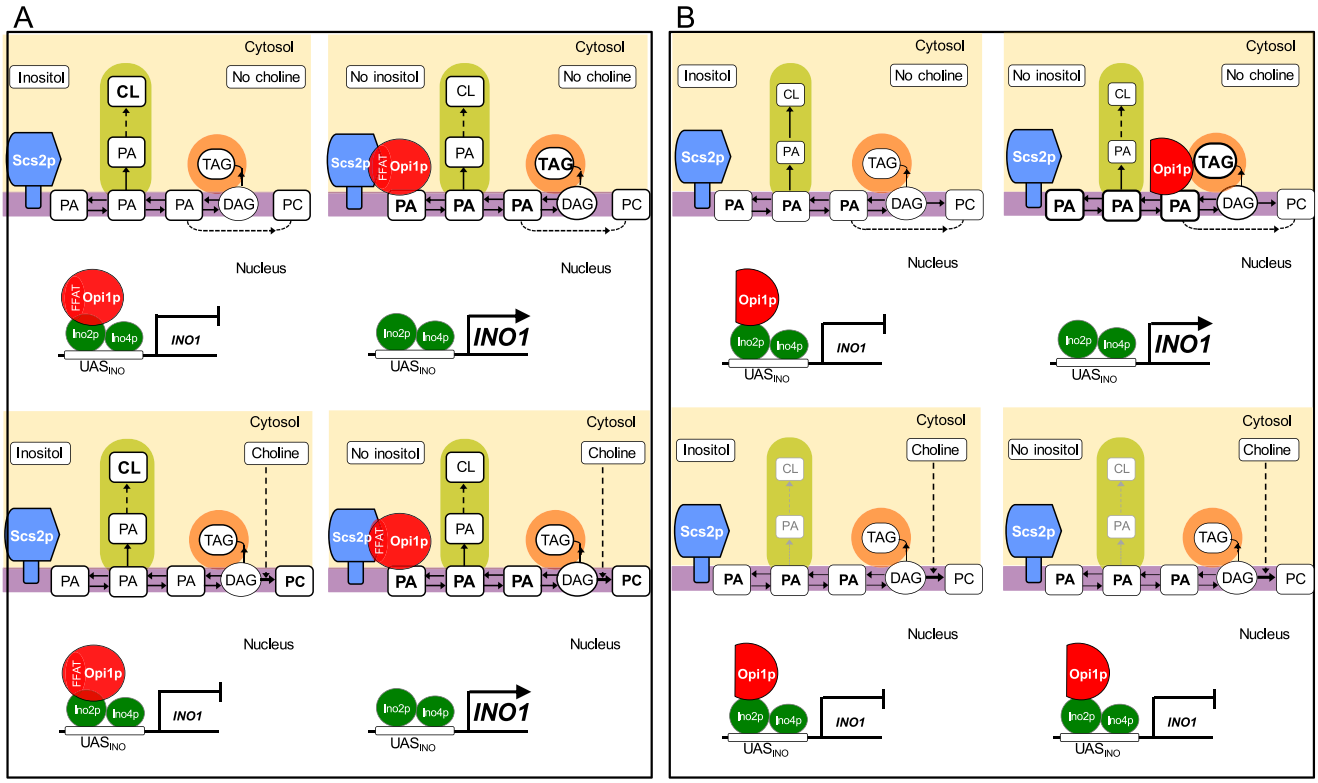

Figure 10. Effect of the Opi1p–Scs2p interaction on lipid metabolism and the regulation of phospholipid biosynthetic genes. *A*, wild-type cells exhibit normal repression and derepression of *INO1* expression in response to changing levels of exogenous inositol. CL content is not affected by inositol in the wild type. Following a shift to medium lacking inositol with or without choline, Opi1p (depicted as a *red circle* with a FFAT domain) exits the nucleus and interacts with both Scs2p and PA in the ER. Moreover, TAG levels increase after the shift to medium lacking both inositol and choline. However, in the presence of choline, DAG consumption increases to synthesize PC, resulting in diminished TAG content. The presence of choline also results in a reduction in CL. *B*, when the *OPI1*^{ffat} strain is shifted to medium lacking inositol, Opi1^{ffat}p (depicted in a *red semicircle*, lacking a FFAT domain) leaves the nucleus and localizes to sites of lipid droplet formation, in contrast to the perinuclear ER, as is the case for Opi1p (as shown in *A*). In addition, in the presence of choline, CL content is also dramatically decreased. However, the presence of choline results in both reduced TAG levels and reduced lipid droplet formation. Under these conditions, the *OPI1*^{ffat} strain is unable to interact with sites of lipid droplet formation in the perinuclear ER and remains in the nucleus, preventing *INO1* expression. *Purple box*, ER; *orange box*, lipid droplet; *green box*, mitochondria; *light yellow box*, cytosol.

(vacuole and mitochondrial patch) resulted in a higher reduction of CL synthesis than disruption of ERMES alone (62). Thus, the residual synthesis of CL, which we observed in both the *scs2*Δ and *OPI1*^{ffat} strains, compared with wild type (Fig. 7), could be the result of compensatory vCLAMP facilitation of PA transfer to mitochondria from the vacuole. Regardless, the low CL levels detected in the *scs2*Δ and *OPI1*^{ffat} strains strongly support the hypothesis that the interaction of Opi1p and Scs2p facilitates optimal transfer of PA from the ER to mitochondria. However, when growing in the presence of choline, CL levels were reduced in all strains, and the relative reduction in CL levels in the presence of choline was proportionally much greater in the wild-type strain than in the *OPI1*^{ffat} and *scs2*Δ strains, in which CL levels were already greatly reduced due to the loss of the Opi1p–Scs2p interaction (Fig. 7). As we discuss below, the presence of exogenous choline exerts distinctly different effects on specific pools of PA in the ER.

The presence of choline alone has a significant impact on TAG content. The substantial reduction in the level of TAG observed in the wild-type strain growing in the presence of choline is consistent with the hypothesis that PC synthesis via the CDP-choline pathway competes directly for a pool of DAG that serves as precursor to TAG synthesis. Also, in contrast to the dramatic increase in PI levels observed in the presence of inositol (Fig. 9), choline is associated with only a modest increase in PC levels in the wild-type strain, regardless of inositol supplementation. These relatively small changes in PC levels in the wild-type strain growing in the presence of choline are consistent with previous reports that choline induces turnover of PC by deacylation, via the Nte1p phospholipase B (63–66). However, in both the wild-type and *OPI1*^{ffat} strains, supplementation with both choline and inositol was associated with a reduction in most neutral lipids, especially TAG. In contrast, most neutral lipids were markedly elevated in the *scs2*Δ strain in I^+C^+ medium, as compared with the other two strains as well as with its own neutral lipid composition in I^+C^- medium. These data are indicative of significant additional perturbations of neutral lipid metabolism related to the total loss of Scs2p function.

A major issue that remains to be discussed is the root cause of the choline-sensitive inositol auxotrophy of the *OPI1*^{ffat} and *scs2*Δ strains. Both strains exhibit Ino$^-$ phenotypes that are more evident both in the presence of choline and at the higher growth temperature of 34 °C (Fig. 2). This phenotype is essentially identical to the phenotype of "choline-sensitive inositol auxotrophy" as originally described in association with the *CSE* mutant used in the isolation of the *SCS2* gene as a high copy suppressor (31). Retention of the Opi1p repressor in the ER requires its interaction with PA in the ER, and this interaction is

essential both for expression of *INO1* and growth of wild-type cells in the absence of inositol (15). Opi1^{ffat}p-GFP in the *OPI1*^{ffat} strain and Opi1p-GFP in the *scs2*Δ strains, respectively, both retain the ability to interact with PA in the ER. However, neither the *OPI1*^{ffat} nor the *scs2*Δ strain has the capacity for direct interaction between Opi1p and Scs2p in the ER. Importantly, after the shift to inositol-free medium in the absence of choline, Opi1^{ffat}p-GFP in the *OPI1*^{ffat} strain exited the nucleus and localized to distinctive puncta associated with synthesis of TAG in lipid droplet formation. Moreover, the level of *INO1* derepression in the *OPI1*^{ffat} strain following the shift from I^+C^- to I^-C^- medium was only slightly lower than that supported by Opi1p in the wild-type strain under the same conditions. Thus, we conclude that the pool of PA associated with lipid droplet formation in the ER, which is created by diversion of PA from PI to increasing TAG synthesis after the shift from I^+C^- to I^-C^- medium, is sufficiently robust to serve as a signal for the exit of Opi1^{ffat}p from the nucleus. However, when choline is present in the absence of inositol, increased PC synthesis competes directly for the pool of DAG derived from PA, a pool of DAG in the ER that also serves as the immediate precursor for TAG. Thus, the presence of choline results in both reduced TAG levels and reduced lipid droplet formation. Under these conditions, the Opi1^{ffat}p in the *OPI1*^{ffat} strain is unable to interact with sites of lipid droplet formation in the perinuclear ER and remains in the nucleus, preventing *INO1* expression. This, indeed, is the root cause of the choline-sensitive inositol auxotrophy shown in Fig. 2.

Experimental procedures

Strains

Yeast strains used are listed in Table 1. The parent strain BY4742 (*MATα*, *his3Δ1*, *leu2Δ0*, *lys2Δ0*, *ura3Δ0*) derived from S288C (67) and mutants derived from BY4742 were used. All strains were maintained on YPD plates (1% yeast extract, 2% bactopeptone, 2% glucose, and 2% agar). Mutations in the FFAT motif (*OPI1*^{ffat}) (residues 200–203 mutated from EFFD to ALLA) within the genomic *OPI1* locus were created using the *delitto perfetto* method (68). The mutated sites are as described by Loewen *et al.* (15). Deletion mutant strains for *PCT1* were generated in wild-type, *scs2*Δ, and *OPI1*^{ffat} strains by PCR-mediated gene replacement, as described previously (69). The plasmid pRS315 was used as a template to generate a PCR fragment for the *PCT1* gene disruption. The entire open reading frame of the *PCT1* gene was replaced with the *LEU2* marker gene. Leucine prototrophs were screened by colony PCR to verify integration at the correct genetic locus.

Construction of strains expressing Opi1p-GFP and Opi1p^{ffat}-GFP fusion proteins tagged at the C terminus of the OPI1 genomic locus

Fusions of GFP to the C termini of wild-type, *scs2*Δ, and *OPI1*^{ffat} strains were constructed by PCR-mediated gene integration at the genomic *OPI1* locus using the template plasmid pFA6a-GFP (S65T)-kanMX6 (a gift from M. Longtine) (69). The insertion of GFP was confirmed by PCR, and expression of genomic Opi1p-GFP and its variants was confirmed by Western blotting.

Analysis of Ino$^-$ phenotypes on solid media

The presence of choline has been shown to increase the severity of Ino$^-$ phenotypes (*i.e.* reduce residual growth in the absence of inositol) in a number of mutant strains in plating assays, including *scs2*Δ (14). Chromatographic assessment of residual choline, performed in our laboratory on samples of agar sourced from several vendors, indicated that all of these agar samples contained varying trace levels of choline (data not shown). However, in our analysis, agar sourced from Sigma contained the lowest residual trace of choline and was therefore used exclusively in all plate assays for assessing Ino$^-$ phenotypes in this study. Yeast strains were grown to mid-logarithmic phase in synthetic complete medium containing 75 μM inositol (I^+ medium), harvested, washed with sterile distilled water, and resuspended in sterile distilled water at a concentration of 1.0 $A_{600\,nm}$/ml. 10-Fold serial dilutions were then spotted onto plates containing 0 μM inositol (I^-) or 75 μM inositol (I^+) with or without 1 mM choline (C^+) and incubated at the indicated temperature of 30 or 34 °C for 3 days.

Protocol for assessing the Pet$^-$ phenotype

The *opi1*Δ mutation was shown to confer the Pet$^-$ phenotype (34), namely the inability to tolerate the loss of the mitochondrial genome (57). Accordingly, we tested the *OPI1*^{ffat} strain for ethidium bromide sensitivity, a phenotype that is associated with complete loss of the mitochondrial genome, following the procedure used by Luévano-Martinez *et al.* (34). In brief, strains were cultured in YPD supplemented with 25 μg/ml filtered sterilized ethidium bromide at 30 °C to an $A_{600\,nm} = 0.5$. At this optical density, samples were subjected to serial dilution in sterile distilled water and spotted onto YPD and YPD plus 25 μg/ml ethidium bromide agar plates. Strains were grown for 2 days on the plates, whereupon the plates were examined for growth conditions under which the Pet$^-$ strains fail to grow.

Protocol for growth in liquid medium and shifting cells from medium containing inositol to medium lacking inositol

All studies on cells grown in liquid medium were conducted at 30 °C. As described by Gaspar *et al.* (43), cells were pregrown overnight in medium containing 75 μM inositol with or without 1 mM choline (*i.e.* I^+C^+ or I^+C^- medium). The following day, cultures were diluted back to $A_{600} = 0.2$ in the same medium at the same temperature and allowed to grow to mid-logarithmic growth phase, $A_{600} = 0.5–0.6$, in I^+C^- or I^+C^+ medium, respectively. Cells were then collected by filtration, washed with I^-C^- or I^-C^+ medium prewarmed to 30 °C, and resuspended in I^-C^- or I^-C^+ medium at the same temperature. Samples were harvested by filtration or centrifugation immediately after 0, 1, 2, and 3 h of growth. Inositol was then reintroduced to the cell cultures at a concentration of 75 μM, and cells were harvested 30 min after inositol readdition. Harvested cells were flash frozen on dry ice after harvesting and stored at −80 °C for RNA extraction. Changes in lipid metabolism and gene expression, as described below, were also measured over the same interval in a strain carrying Opi1-GFP (wild type; YCY3) and compared with its parent, BY4742 (Table 1), expressing untagged Opi1p. The level of expression of *INO1* at

each time point was not statistically different in the BY4742 strain, in comparison with the YCY3 strain at any time point before or after a shift from I^+C^- to I^-C^- medium or from I^+C^+ to I^-C^+ medium or following the readdition of inositol (data not shown). On this basis, the YCY3 strain was used as the "wild-type" control for analysis of gene expression, Opi1p localization, and lipid metabolism in response to inositol and choline supplementation.

RNA isolation and RT-PCR analysis

Strains were pregrown as described above in I^+C^- or I^+C^+ liquid medium at 30 °C and then shifted to I^-C^- or I^-C^+ medium, respectively, maintaining constant growth temperature. Total RNA was isolated using the RNeasy® minikit, including a DNA digestion with an RNase-free DNase set (both from Qiagen). 1 μg of RNA was transcribed into cDNA using oligo$(dT)_{12-18}$ primer (0.5 μg), PCR grade dNTP mix (0.5 μM), First Strand Buffer (1×), DTT (10 mM), and 100 units of Maxima™ reverse transcriptase (Fermentas). Real-time PCR was performed on a StepOnePlus™ real-time PCR system (Applied Biosystems) using Maxima® probe/ROX qPCR Master Mix, No AmpErase® UNG (Applied Biosystems), and the following TaqMan® probes and primers: *INO1*, TaqMan® probe, 5′-FAM-CTGTTG CCC ATG GTT AGC CCA AAC G-TAMRA-3′; forward primer, 5′-GGA ATG ACG TTT ATG CTC CTT TTA A-3′; reverse primer, 5′-GTC CCA ACC AGA GAC GAC AAA-3′; *ACT1*, TaqMan® probe, 5′-FAM-TGC AAA CCG CTG CTC AAT CTT CTT CAAT-TAMRA-3′; forward primer, 5′-CGC CTT GGA CTT CGA ACA AG-3′; reverse primer, 5′-GAC CAT CTG GAA GTT CGT AGG ATT-3′. The *ACT1* gene served as an internal standard for normalization.

In brief, the reaction mix in a volume of 25 μl consisted of 0.5 μM primers, 0.2 μM TaqMan® probe, 1× Master Mix, and 10 ng of cDNA. All reactions were performed in technical duplicate. Non-template control (10 ng of RNA) and non-reaction control (RNase-free water) were routinely performed. The thermal program for the PCR included stage 1 (95 °C for 10 min), stage 2 (95 °C for 0.5 min and 60 °C for 1 min for a total of 40 cycles), and stage 3 (hold at 4 °C). Relative quantitation was done using the $\Delta\Delta Ct$ method (see the StepOnePlus™ user manual, Applied Biosystems). The $\Delta\Delta Ct$ represents the change in mRNA expression after *ACT1* normalization relative to the wild-type control calculated as follows: $2-(Gene\ Ct_x - ACT1\ Ct_x) - (Gene\ Ct_{cr} - ACT1\ Ct_{cr})$, where *Gene* represents the mRNA under study (*INO1*), *x* refers to the strain from which the mRNA to be tested was derived (*i.e.* wild type or mutant), and *cr* refers to the control mRNA, the value of which was derived from the level of mRNA in the BY4742 parent strain, pregrown as described above in I^+ medium at 30 °C, shifted to I− medium at the same temperature at time 0 h. The *Ct* (cycle threshold) is defined as the number of cycles required for the fluorescent signal to cross the threshold (*i.e.* to exceed background level). Each RT-PCR experiment was performed in triplicate.

Fluorescence microscopy

Wild type, *scs2*Δ, and $OPI1^{ffat}$ cells, expressing genomic or plasmid versions of GFP-tagged *OPI1* or $OPI1^{ffat}$, were grown overnight, as described above, at 30 °C in I^+C^- or I^+C^+ medium. Before microscopy, overnight cultures were diluted to $A_{600} = 0.2$ and allowed to continue to grow to mid-logarithmic phase in I^+C^- or I^+C^+ medium at 30 °C. After reaching $A_{600} = 0.5–0.6$, cultures were shifted, as described above, to I^-C^- or I^-C^+ medium, respectively, and allowed to grow for 2 h ($A_{600} = 0.8–1.0$) for single time point observations or to 4–5 h ($A_{600} = 1.5–2$) for time course observations. Cells were then concentrated to OD = 12.5 by centrifugation, and 3.5-μl samples of concentrated cultures were subjected to deconvolution fluorescence microscopy using a Deltaversion RT microscopy system (Applied Precision, LLC). Cells were viewed using a X71 Olympus microscope equipped with a PlanApo 100× objective (1.35 numeric aperture, Olympus), FITC, and rhodamine filters and a Cool Snap HQ digital camera (Photometrics). GFP images were acquired with the FITC filter set, and RFP/mCherry images were acquired with the RD-TR-PE filter set. Five or six *z*-sections from each strain were inspected. The acquired images were deconvolved using soft-WoRX version 3.5.0 software (Applied Precision, LLC). The colocalization of GFP-Opi1p or GFP-$Opi1p^{ffat}$ with the lipid droplet marker RFP-Erg6p (Table 1) was analyzed with PCC (48) in soft-WoRX version 3.5.0. The number of prominent punctate structures associated with $Opi1p^{ffat}$-GFP was manually counted in 50 cells by scanning through the *z*-sections.

Phospholipid composition assessed by [^{32}P]orthophosphate steady-state labeling

Changes in the composition of cellular phospholipids were determined over a time course of 3 h following a shift of actively growing cells from medium containing inositol to medium lacking inositol, followed by subsequent reintroduction of inositol into the medium. For this purpose, cells were grown overnight, as described above, in I^+C^- or I^+C^+ medium at 30 °C in the presence of 10 μCi/ml [^{32}P]orthophosphate. The following day, cultures were diluted to $A_{600\ nm} = 0.1$ in I^+C^- or I^+C^+ medium at 30 °C maintaining label at 10 μCi/ml [^{32}P] orthophosphate and allowed to grow to mid-logarithmic phase ($A_{600} = 0.5–0.6$). At this cell density, each culture was divided in half. One-half of each culture was filtered, washed with prewarmed medium containing inositol, and resuspended in I^+C^- or I^+C^+ medium at 30 °C, maintaining label at 10 μCi/ml [^{32}P]orthophosphate. The other half was also filtered and then washed with prewarmed medium lacking inositol and resuspended in I^-C^- or I^-C^+ medium at 30 °C maintaining label at 10 μCi/ml [^{32}P]orthophosphate. Samples from each culture were taken at 2 or 3 h following the shift. Labeled lipids were extracted as described by Gaspar *et al.* (50). The individual phospholipid species were resolved by two-dimensional thin layer chromatography (50).

For the assessment of CL content, lipids were labeled with [^{32}P]orthophosphate and extracted, as described above, and the lipid extract was analyzed by one-dimensional thin layer chromatography according to the method developed by Vaden *et al.* (70). Briefly, Sigma-Aldrich Silicagel on TLC plates (layer thickness 250 μm) were dipped in 1.8% boric acid prepared in 100% ethanol, dried for 5 min, and baked for 15 min at 100 °C. Phospholipids were separated using the solvent system chloroform/ethanol/water/triethylamine (30/35/7/35, v/v/v/v) for at least 2 h. Phospholipid identity was based on the mobility of known

standards and quantified on a STORM 860 PhosphorImager (Amersham Biosciences).

Neutral lipid composition assessed by steady-state labeling with [^{14}C]acetate

Cells were grown as described above for ^{32}P steady-state labeling, except that they were labeled in the presence of 2 μCi/ml [1-^{14}C]acetate (specific activity, 57 mCi/mmol) to steady state in I^+C^- or I^+C^+ medium at 30 °C and then shifted to I^-C^- or I^-C^+ at 30 °C medium respectively, maintaining label, as described above, at 2 μCi/ml [1-^{14}C]acetate. Changes in neutral lipid composition were monitored over a set time course of 2 or 3 h after the shift to medium lacking inositol, followed by inositol readdition. Samples were taken at 0 and 2 h following the shift to I^-C^- or I^-C^+ medium. 5-ml samples were mixed with 0.5 ml of 50% trichloroacetic acid and allowed to stand on ice for 20 min. Lipids were extracted and analyzed as described by Gaspar *et al.* (50). Labeled lipids on the chromatograms were quantified on a STORM 860 PhosphorImager (Amersham Biosciences), and metabolites were identified as described previously (50).

Author contributions—M. L. G., Y.-F. C., and S. A. J. performed the experiments and prepared the manuscript. M. A. performed experiments. S. A. H. directed the research and contributed to the preparation of the manuscript.

References

1. Bachhawat, N., Ouyang, Q., and Henry, S. A. (1995) Functional characterization of an inositol-sensitive upstream activation sequence in yeast: a cis-regulatory element responsible for inositol-choline mediated regulation of phospholipid biosynthesis. *J. Biol. Chem.* **270,** 25087–25095
2. Carman, G. M., and Henry, S. A. (1999) Phospholipid biosynthesis in the yeast *Saccharomyces cerevisiae* and interrelationship with other metabolic processes. *Prog. Lipid Res.* **38,** 361–399
3. Henry, S. A., Gaspar, M. L., and Jesch, S. A. (2014) The response to inositol: regulation of glycerolipid metabolism and stress response signaling in yeast. *Chem. Phys. Lipids* **180,** 23–43
4. Henry, S. A., Kohlwein, S. D., and Carman, G. M. (2012) Metabolism and regulation of glycerolipids in the yeast *Saccharomyces cerevisiae*. *Genetics* **190,** 317–349
5. Jesch, S. A., Zhao, X., Wells, M. T., and Henry, S. A. (2005) Genome-wide analysis reveals inositol, not choline, as the major effector of Ino2p-Ino4p and unfolded protein response target gene expression in yeast. *J. Biol. Chem.* **280,** 9106–9118
6. Hirsch, J. P., and Henry, S. A. (1986) Expression of the *Saccharomyces cerevisiae* inositol-1-phosphate synthase (INO1) gene is regulated by factors that affect phospholipid synthesis. *Mol. Cell. Biol.* **6,** 3320–3328
7. Jesch SAa, H., SA. (2005) Yeast inositol phospholipids: synthesis, regulation and involvement in membrane trafficking and lipid signaling. in *Cell Biology and Dynamics of Yeast Lipids* (Daum, G., ed.) pp. 105–131, Research Signpost, Kerala, India
8. Santiago, T. C., and Mamoun, C. B. (2003) Genome expression analysis in yeast reveals novel transcriptional regulation by inositol and choline and new regulatory functions for Opi1p, Ino2p, and Ino4p. *J. Biol. Chem.* **278,** 38723–38730
9. Schüller, H. J., Hahn, A., Tröster, F., Schütz, A., and Schweizer, E. (1992) Coordinate genetic control of yeast fatty acid synthase genes FAS1 and FAS2 by an upstream activation site common to genes involved in membrane lipid biosynthesis. *EMBO J.* **11,** 107–114
10. Donahue, T. F., and Henry, S. A. (1981) *myo*-Inositol-1-phosphate synthase: characteristics of the enzyme and identification of its structural gene in yeast. *J. Biol. Chem.* **256,** 7077–7085
11. Jesch, S. A., Liu, P., Zhao, X., Wells, M. T., and Henry, S. A. (2006) Multiple endoplasmic reticulum-to-nucleus signaling pathways coordinate phospholipid metabolism with gene expression by distinct mechanisms. *J. Biol. Chem.* **281,** 24070–24083
12. Culbertson, M. R., and Henry, S. A. (1975) Inositol-requiring mutants of *Saccharomyces cerevisiae*. *Genetics* **80,** 23–40
13. Ambroziak, J., and Henry, S. A. (1994) INO2 and INO4 gene products, positive regulators of phospholipid biosynthesis in *Saccharomyces cerevisiae*, form a complex that binds to the INO1 promoter. *J. Biol. Chem.* **269,** 15344–15349
14. Villa-García, M. J., Choi, M. S., Hinz, F. I., Gaspar, M. L., Jesch, S. A., and Henry, S. A. (2011) Genome-wide screen for inositol auxotrophy in *Saccharomyces cerevisiae* implicates lipid metabolism in stress response signaling. *Mol. Genet. Genomics* **285,** 125–149
15. Loewen, C. J., Gaspar, M. L., Jesch, S. A., Delon, C., Ktistakis, N. T., Henry, S. A., and Levine, T. P. (2004) Phospholipid metabolism regulated by a transcription factor sensing phosphatidic acid. *Science* **304,** 1644–1647
16. Wagner, C., Dietz, M., Wittmann, J., Albrecht, A., and Schüller, H. J. (2001) The negative regulator Opi1 of phospholipid biosynthesis in yeast contacts the pleiotropic repressor Sin3 and the transcriptional activator Ino2. *Mol. Microbiol.* **41,** 155–166
17. Kagiwada, S., Hosaka, K., Murata, M., Nikawa, J., and Takatsuki, A. (1998) The *Saccharomyces cerevisiae* SCS2 gene product, a homolog of a synaptobrevin-associated protein, is an integral membrane protein of the endoplasmic reticulum and is required for inositol metabolism. *J. Bacteriol.* **180,** 1700–1708
18. Kagiwada, S., and Zen, R. (2003) Role of the yeast VAP homolog, Scs2p, in INO1 expression and phospholipid metabolism. *J. Biochem.* **133,** 515–522
19. Loewen, C. J., Roy, A., and Levine, T. P. (2003) A conserved ER targeting motif in three families of lipid binding proteins and in Opi1p binds VAP. *EMBO J.* **22,** 2025–2035
20. Loewen, C. J., and Levine, T. P. (2005) A highly conserved binding site in vesicle-associated membrane protein-associated protein (VAP) for the FFAT motif of lipid-binding proteins. *J. Biol. Chem.* **280,** 14097–14104
21. Murphy, S. E., and Levine, T. P. (2016) VAP, a versatile access point for the endoplasmic reticulum: review and analysis of FFAT-like motifs in the VAPome. *Biochim. Biophys. Acta* **1861,** 952–961
22. Holthuis, J. C., and Menon, A. K. (2014) Lipid landscapes and pipelines in membrane homeostasis. *Nature* **510,** 48–57
23. Levine, T. (2004) Short-range intracellular trafficking of small molecules across endoplasmic reticulum junctions. *Trends Cell Biol.* **14,** 483–490
24. Prinz, W. A. (2014) Bridging the gap: membrane contact sites in signaling, metabolism, and organelle dynamics. *J. Cell Biol.* **205,** 759–769
25. Stefan, C. J., Manford, A. G., Baird, D., Yamada-Hanff, J., Mao, Y., and Emr, S. D. (2011) Osh proteins regulate phosphoinositide metabolism at ER-plasma membrane contact sites. *Cell* **144,** 389–401
26. Manford, A. G., Stefan, C. J., Yuan, H. L., Macgurn, J. A., and Emr, S. D. (2012) ER-to-plasma membrane tethering proteins regulate cell signaling and ER morphology. *Dev. Cell* **23,** 1129–1140
27. Gavin, A. C., Bösche, M., Krause, R., Grandi, P., Marzioch, M., Bauer, A., Schultz, J., Rick, J. M., Michon, A. M., Cruciat, C. M., Remor, M., Höfert, C., Schelder, M., Brajenovic, M., Ruffner, H., *et al.* (2002) Functional organization of the yeast proteome by systematic analysis of protein complexes. *Nature* **415,** 141–147
28. Levine, T. P., and Munro, S. (2001) Dual targeting of Osh1p, a yeast homologue of oxysterol-binding protein, to both the Golgi and the nucleus-vacuole junction. *Mol. Biol. Cell* **12,** 1633–1644
29. Loewen, C. J., Young, B. P., Tavassoli, S., and Levine, T. P. (2007) Inheritance of cortical ER in yeast is required for normal septin organization. *J. Cell Biol.* **179,** 467–483
30. Wilson, J. D., Thompson, S. L., and Barlowe, C. (2011) Yet1p-Yet3p interacts with Scs2p-Opi1p to regulate ER localization of the Opi1p repressor. *Mol. Biol. Cell* **22,** 1430–1439
31. Hosaka, K., Nikawa, J., Kodaki, T., and Yamashita, S. (1992) A dominant mutation that alters the regulation of INO1 expression in *Saccharomyces cerevisiae*. *J. Biochem.* **111,** 352–358

32. Skehel, P. A., Martin, K. C., Kandel, E. R., and Bartsch, D. (1995) A VAMP-binding protein from Aplysia required for neurotransmitter release. *Science* **269,** 1580–1583
33. Greenberg, M. L., Goldwasser, P., and Henry, S. A. (1982) Characterization of a yeast regulatory mutant constitutive for synthesis of inositol-1-phosphate synthase. *Mol. Gen. Genet.* **186,** 157–163
34. Luévano-Martinez, L. A., Appolinario, P., Miyamoto, S., Uribe-Carvajal, S., and Kowaltowski, A. J. (2013) Deletion of the transcriptional regulator opi1p decreases cardiolipin content and disrupts mitochondrial metabolism in *Saccharomyces cerevisiae*. *Fungal Genet. Biol.* **60,** 150–158
35. Baile, M. G., Lu, Y. W., and Claypool, S. M. (2014) The topology and regulation of cardiolipin biosynthesis and remodeling in yeast. *Chem. Phys. Lipids* **179,** 25–31
36. Connerth, M., Tatsuta, T., Haag, M., Klecker, T., Westermann, B., and Langer, T. (2012) Intramitochondrial transport of phosphatidic acid in yeast by a lipid transfer protein. *Science* **338,** 815–818
37. Kornmann, B., Currie, E., Collins, S. R., Schuldiner, M., Nunnari, J., Weissman, J. S., and Walter, P. (2009) An ER-mitochondria tethering complex revealed by a synthetic biology screen. *Science* **325,** 477–481
38. Osman, C., Haag, M., Potting, C., Rodenfels, J., Dip, P. V., Wieland, F. T., Brügger, B., Westermann, B., and Langer, T. (2009) The genetic interactome of prohibitins: coordinated control of cardiolipin and phosphatidylethanolamine by conserved regulators in mitochondria. *J. Cell Biol.* **184,** 583–596
39. Nikawa, J., Murakami, A., Esumi, E., and Hosaka, K. (1995) Cloning and sequence of the SCS2 gene, which can suppress the defect of INO1 expression in an inositol auxotrophic mutant of *Saccharomyces cerevisiae*. *J. Biochem.* **118,** 39–45
40. Chao, J. T., Wong, A. K., Tavassoli, S., Young, B. P., Chruscicki, A., Fang, N. N., Howe, L. J., Mayor, T., Foster, L. J., and Loewen, C. J. (2014) Polarization of the endoplasmic reticulum by ER-septin tethering. *Cell* **158,** 620–632
41. Tsukagoshi, Y., Nikawa, J., and Yamashita, S. (1987) Molecular cloning and characterization of the gene encoding cholinephosphate cytidylyltransferase in *Saccharomyces cerevisiae*. *Eur. J. Biochem.* **169,** 477–486
42. Weiss, S. B., Smith, S. W., and Kennedy, E. P. (1958) The enzymatic formation of lecithin from cytidine diphosphate choline and D-1,2-diglyceride. *J. Biol. Chem.* **231,** 53–64
43. Gaspar, M. L., Hofbauer, H. F., Kohlwein, S. D., and Henry, S. A. (2011) Coordination of storage lipid synthesis and membrane biogenesis: evidence for cross-talk between triacylglycerol metabolism and phosphatidylinositol synthesis. *J. Biol. Chem.* **286,** 1696–1708
44. Han, S., Binns, D. D., Chang, Y. F., and Goodman, J. M. (2015) Dissecting seipin function: the localized accumulation of phosphatidic acid at ER/LD junctions in the absence of seipin is suppressed by Sei1p(DeltaNterm) only in combination with Ldb16p. *BMC Cell Biol.* **16,** 29
45. Kurat, C. F., Wolinski, H., Petschnigg, J., Kaluarachchi, S., Andrews, B., Natter, K., and Kohlwein, S. D. (2009) Cdk1/Cdc28-dependent activation of the major triacylglycerol lipase Tgl4 in yeast links lipolysis to cell-cycle progression. *Mol. Cell* **33,** 53–63
46. Athenstaedt, K., Zweytick, D., Jandrositz, A., Kohlwein, S. D., and Daum, G. (1999) Identification and characterization of major lipid particle proteins of the yeast *Saccharomyces cerevisiae*. *J. Bacteriol.* **181,** 6441–6448
47. Curwin, A. J., Fairn, G. D., and McMaster, C. R. (2009) Phospholipid transfer protein Sec14 is required for trafficking from endosomes and regulates distinct trans-Golgi export pathways. *J. Biol. Chem.* **284,** 7364–7375
48. Manders, E. M., Stap, J., Brakenhoff, G. J., van Driel, R., and Aten, J. A. (1992) Dynamics of three-dimensional replication patterns during the S-phase, analysed by double labelling of DNA and confocal microscopy. *J. Cell Sci.* **103**, 857–862
49. Grillitsch, K., Connerth, M., Köfeler, H., Arrey, T. N., Rietschel, B., Wagner, B., Karas, M., and Daum, G. (2011) Lipid particles/droplets of the yeast *Saccharomyces cerevisiae* revisited: lipidome meets proteome. *Biochim. Biophys. Acta* **1811,** 1165–1176
50. Gaspar, M. L., Aregullin, M. A., Jesch, S. A., and Henry, S. A. (2006) Inositol induces a profound alteration in the pattern and rate of synthesis and turnover of membrane lipids in *Saccharomyces cerevisiae*. *J. Biol. Chem.* **281,** 22773–22785
51. Gaspar, M. L., Jesch, S. A., Viswanatha, R., Antosh, A. L., Brown, W. J., Kohlwein, S. D., and Henry, S. A. (2008) A block in endoplasmic reticulum-to-Golgi trafficking inhibits phospholipid synthesis and induces neutral lipid accumulation. *J. Biol. Chem.* **283,** 25735–25751
52. Sandager, L., Gustavsson, M. H., Ståhl, U., Dahlqvist, A., Wiberg, E., Banas, A., Lenman, M., Ronne, H., and Stymne, S. (2002) Storage lipid synthesis is non-essential in yeast. *J. Biol. Chem.* **277,** 6478–6482
53. Tatsuta, T., Scharwey, M., and Langer, T. (2014) Mitochondrial lipid trafficking. *Trends Cell Biol.* **24,** 44–52
54. Tamura, Y., Harada, Y., Nishikawa, S., Yamano, K., Kamiya, M., Shiota, T., Kuroda, T., Kuge, O., Sesaki, H., Imai, K., Tomii, K., and Endo, T. (2013) Tam41 is a CDP-diacylglycerol synthase required for cardiolipin biosynthesis in mitochondria. *Cell Metab.* **17,** 709–718
55. Tamura, Y., Sesaki, H., and Endo, T. (2014) Phospholipid transport via mitochondria. *Traffic* **15,** 933–945
56. Watanabe, Y., Tamura, Y., Kawano, S., and Endo, T. (2015) Structural and mechanistic insights into phospholipid transfer by Ups1-Mdm35 in mitochondria. *Nat. Commun.* **6,** 7922
57. Dunn, C. D., Lee, M. S., Spencer, F. A., and Jensen, R. E. (2006) A genome-wide screen for petite-negative yeast strains yields a new subunit of the i-AAA protease complex. *Mol. Biol. Cell* **17,** 213–226
58. Kannan, M., Riekhof, W. R., and Voelker, D. R. (2015) Transport of phosphatidylserine from the endoplasmic reticulum to the site of phosphatidylserine decarboxylase2 in yeast. *Traffic* **16,** 123–134
59. Di Bartolomeo, F., Wagner, A., and Daum, G. (2017) Cell biology, physiology and enzymology of phosphatidylserine decarboxylase. *Biochim. Biophys. Acta* **1862,** 25–38
60. Greenberg, M. L., Reiner, B., and Henry, S. A. (1982) Regulatory mutations of inositol biosynthesis in yeast: isolation of inositol-excreting mutants. *Genetics* **100,** 19–33
61. AhYoung, A. P., Jiang, J., Zhang, J., Khoi Dang, X., Loo, J. A., Zhou, Z. H., and Egea, P. F. (2015) Conserved SMP domains of the ERMES complex bind phospholipids and mediate tether assembly. *Proc. Natl. Acad. Sci. U.S.A.* **112,** E3179–E3188
62. Elbaz-Alon, Y., Rosenfeld-Gur, E., Shinder, V., Futerman, A. H., Geiger, T., and Schuldiner, M. (2014) A dynamic interface between vacuoles and mitochondria in yeast. *Dev. Cell* **30,** 95–102
63. Dowd, S. R., Bier, M. E., and Patton-Vogt, J. L. (2001) Turnover of phosphatidylcholine in *Saccharomyces cerevisiae*: the role of the CDP-choline pathway. *J. Biol. Chem.* **276,** 3756–3763
64. Fernández-Murray, J. P., and McMaster, C. R. (2005) Glycerophosphocholine catabolism as a new route for choline formation for phosphatidylcholine synthesis by the Kennedy pathway. *J. Biol. Chem.* **280,** 38290–38296
65. Fernández-Murray, J. P., and McMaster, C. R. (2007) Phosphatidylcholine synthesis and its catabolism by yeast neuropathy target esterase 1. *Biochim. Biophys. Acta* **1771,** 331–336
66. Zaccheo, O., Dinsdale, D., Meacock, P. A., and Glynn, P. (2004) Neuropathy target esterase and its yeast homologue degrade phosphatidylcholine to glycerophosphocholine in living cells. *J. Biol. Chem.* **279,** 24024–24033
67. Brachmann, C. B., Davies, A., Cost, G. J., Caputo, E., Li, J., Hieter, P., and Boeke, J. D. (1998) Designer deletion strains derived from *Saccharomyces cerevisiae* S288C: a useful set of strains and plasmids for PCR-mediated gene disruption and other applications. *Yeast* **14,** 115–132
68. Storici, F., Lewis, L. K., and Resnick, M. A. (2001) *In vivo* site-directed mutagenesis using oligonucleotides. *Nat. Biotechnol.* **19,** 773–776
69. Longtine, M. S., McKenzie, A., 3rd, Demarini, D. J., Shah, N. G., Wach, A., Brachat, A., Philippsen, P., and Pringle, J. R. (1998) Additional modules for versatile and economical PCR-based gene deletion and modification in *Saccharomyces cerevisiae*. *Yeast* **14,** 953–961
70. Vaden, D. L., Gohil, V. M., Gu, Z., and Greenberg, M. L. (2005) Separation of yeast phospholipids using one-dimensional thin-layer chromatography. *Anal. Biochem.* **338,** 162–164
71. Petschnigg, J., Wolinski, H., Kolb, D., Zellnig, G., Kurat, C. F., Natter, K., and Kohlwein, S. D. (2009) Good fat, essential cellular requirements for triacylglycerol synthesis to maintain membrane homeostasis in yeast. *J. Biol. Chem.* **284,** 30981–30993
72. Rue, S. M., Mattei, S., Saksena, S., and Emr, S. D. (2008) Novel Ist1-Did2 complex functions at a late step in multivesicular body sorting. *Mol. Biol. Cell* **19,** 475–484